T.R.

GEBZE TECHNICAL UNIVERSITY

GRADUATE SCHOOL OF NATURAL AND APPLIED SCIENCES

TEMPOROSPATIAL METABOLIC MODELLING OF PSEUDOMONAS AERUGINOSA AND STAPHYLOCOCCUS AUREUS ON A CHRONIC WOUND

TUĞBERK TALAK

A THESIS SUBMITTED FOR THE DEGREE OF

MASTER OF SCIENCE

DEPARTMENT OF BIOENGINEERING

BIOINFORMATICS AND SYSTEMS BIOLOGY PROGRAMME

GEBZE

2021

T.R.

GEBZE TECHNICAL UNIVERSITY

GRADUATE SCHOOL OF NATURAL AND APPLIED SCIENCES

TEMPOROSPATIAL METABOLIC MODELLING OF PSEUDOMONAS AERUGINOSA AND STAPHYLOCOCCUS AUREUS ON A CHRONIC WOUND

TUĞBERK TALAK

A THESIS SUBMITTED FOR THE DEGREE OF

MASTER OF SCIENCE

DEPARTMENT OF BIOENGINEERING

BIOINFORMATICS AND SYSTEMS BIOLOGY PROGRAMME

THESIS SUPERVISOR

ASSIST. PROF. DR. PINAR PİR

GEBZE

2021

T.C.
GEBZE TEKNİK ÜNİVERSİTESİ
FEN BİLİMLERİ ENSTİTÜSÜ

KRONIK BİR YARADA PSEUDOMONAS AERUGINOSA VE STAPHYLOCOCCUS AUREUS'UN ZAMAN-MEKANSAL METABOLIK MODELLENMESI

TUĞBERK TALAK
YÜKSEK LİSANS TEZİ
BİYOMÜHENDİSLİK ANABİLİM DALI
BİYOİNFORMATİK VE SİSTEM BİYOLOJİSİ PROGRAMI

DANIŞMANI
DR. ÖĞR. ÜYESI PINAR PİR

GEBZE
2021

GEBZE TEKNİK ÜNİVERSİTESİ	YÜKSEK LİSANS JÜRİ ONAY FORMU

GTÜ Fen Bilimleri Enstitüsü Yönetim Kurulu'nun 12/08/2021 tarih ve 2021/36 sayılı kararıyla oluşturulan jüri tarafından 05/11/2021 tarihinde tez savunma sınavı yapılan Tuğberk Talak'ın tez çalışması Biyomühendislik Anabilim Dalı Biyoinformatik ve Sistem Biyolojisi programı YÜKSEK LİSANS tezi olarak kabul edilmiştir.

JÜRİ

ÜYE
(TEZ DANIŞMANI) : Dr. Öğr. Üyesi Pınar PİR

ÜYE : Doç. Dr. Tunahan ÇAKIR

ÜYE : Prof. Dr. Kazım Yalçın ARĞA

ONAY

Gebze Teknik Üniversitesi Fen Bilimleri Enstitüsü Yönetim Kurulu'nun
…..…/…..…/..…..… tarih ve ……/…….. sayılı kararı.

İMZA/MÜHÜR

SUMMARY

Attached to a surface, certain microorganisms can coat their population within extracellular polymeric substances (EPS) which is called a biofilm. For bacteria, how these organisms understand the amount of population around them is explained by a mechanism called Quorum Sensing (QS). Being built after a certain threshold of QS signals, biofilms may provide extra resistance to these organisms from outside effects, while within the substance, organisms may have both beneficial and harmful effects on one another. P. aeruginosa and S. aureus are two such bacteria that are commonly observed in hard to cure human diseases, such as lung infections and chronic wounds. In order to reveal mechanisms behind these infections, both single and multi-species growth models are established. Genome-scale metabolic networks (GMNs) which contain information about genes, reactions and metabolites of given species are used in these models. Firstly, to mimic conditions of blood serum leaking into wounds in normal and diabetic cases, blood concentrations are taken from "The Human Metabolome Database" (HMDB) and are used to create a dynamic environment in Python via discretized diffusion equations. These conditions define exchanges of GMNs of both bacteria, helping simulate dynamic Flux Balance Analysis (dFBA). During simulations, single-species biofilms on regular and chronic wounds as well as impaired QS effects are studied. In multi-species trials, effects of initial points of simulations and different levels of hindering effects of P. aeruginosa on S. aureus are also studied. All these growth maps revealed outcomes and representations consistent with the literature, giving way to further study and decompose mechanisms which may bring further development in medicine to fight these infections.

Key Words: Biofilm, Pseudomonas Aeruginosa, Staphylococcus Aureus, Temporospatial Modelling, Discretized Diffusion, Multiscale Modeling, Genome-Scale Metabolic Networks, Quorum Sensing, Flux Balance Analysis

ÖZET

Bir yüzeye bağlı olan belirli bazı mikroorganizmalar, biyofilm adı verilen hücre dışı polimerik maddeler (EPS) ile kendilerini kaplayabilmektedir. Bakteriler için, bu organizmaların etraflarındaki popülasyon miktarını nasıl anladıkları, Quorum Sensing (QS) adı verilen bir mekanizma ile açıklamaktadır. Belirli bir QS sinyali eşiğinin aşılması ile oluşturulmaya başlayan biyofilmler, bu organizmalara dış etkilerden ekstra direnç sağlayabilirken, madde içindeki organizmaların birbirleri üzerinde hem yararlı hem de zararlı etkileri gözlemlenmektedir. P. aeruginosa ve S. aureus, akciğer enfeksiyonları ve kronik yaralar gibi tedavisi zor hastalıklarında yaygın olarak görülen iki bakteri türüdür. Bu enfeksiyonların arkasındaki mekanizmaları ortaya çıkarmak için hem tek hem de çok tür içeren büyüme modelleri oluşturulmuştur. Bu büyüme modellerde, belirli türlerin genleri, reaksiyonları ve metabolitleri hakkında bilgi içeren genom ölçekli metabolik ağlar (GMNs) kullanılır. İlk olarak, normal ve diyabetik vakalarda yaralara sızan kan serumu durumlarını simüle etmek için “The Human Metabolome Database” (HMDB)'den kan konsantrasyonları alınıp ayrıklaştırılmış difüzyon denklemleri aracılığıyla Python'da dinamik bir ortam oluşturmak için kullanılır. Bu koşullar, her iki bakterinin GMN'lerinin metabolit alışverişlerini tanımlayarak dinamik Akı Dengesi Analizini (dFBA) simüle etmeye yardımcı olur. Simülasyonlar sırasında, normal ve kronik yaralar üzerindeki tek tür içeren biyofilmlerin yanı sıra bozulmuş QS etkileri incelenmiştir. Çoklu tür denemelerinde, simülasyonların başlangıç noktalarının etkileri ve P. aeruginosa'nın S. aureus üzerindeki baskılayıcı etkileri farklı seviyelerde de incelenmiştir. Tüm bu büyüme haritaları, bu enfeksiyonlarla savaşmak için tıpta daha fazla gelişme sağlayabilecek mekanizmaların araştırılmasına ve ayrıştırılmasına olanak sağlayan, literatürle uyumlu sonuçları ve simülasyonları ortaya koymaktadır.

Anahtar Kelimeler: Biyofilm, Pseudomonas Aeruginosa, Staphylococcus Aureus, Zaman-Mekansal Modelleme, Ayrıklaştırılmış Difüzyon, Çok Ölçekli Modelleme, Genom Ölçekli Metabolik Ağlar, Çoğunluk Algılama, Akı Dengesi Analizi

ACKNOWLEDGEMENTS

I would like to express my sincere gratitude to my supervisor Asst. Prof. Pınar Pir for her valuable insight and unshakable backing, teaching me how to start flying over the boundless horizon of systems biology. I like to thank Assoc. Prof. Tunahan Çakır and Prof. Dr. Kazım Yalçın Arğa for broadening my view on my thesis, their critique and comments were the most treasured.

I want to express my joyful gratitude to Cem Yaşa, Neşe Şen, Oğuzhan Kızılçım, and Kadir Kocabaş, for without their support, this thesis would not be complete.

I am grateful that I had the chance to be part of the Computational Systems Biology Group at Gebze Technical University, for my colleagues were the most wholesome addition to my life, bringing joy and wonder.

And my family, their constant support and encouragement are what made this journey possible.

TABLE of CONTENTS

	Page
SUMMARY	v
ÖZET	vi
ACKNOWLEDGEMENTS	vii
TABLE of CONTENTS	viii
LIST of ABBREVIATIONS and ACRONYMS	x
LIST of FIGURES	xi
LIST of TABLES	xii
1. INTRODUCTION	1
1.1. Biofilms	1
1.1.1. Biofilm Heterogeneity	3
1.1.2. Mono- and Multi-Species Biofilms	3
1.1.3. Spatial Organization of Mixed-Species Biofilm	5
1.1.4. Quorum Sensing (QS)	6
1.2. Chronic Wounds and Biofilms	8
1.2.1. Pseudomonas aeruginosa	9
1.2.2. Staphylococcus aureus	10
1.2.3. Two Species Interaction	11
1.3. Multi-Scale Modelling	11
1.3.1. Systems Biology	13
1.3.2. Genome-Scale Metabolic Networks (GMNs)	13
1.3.3. Modelling Approaches	15
1.3.4. Modelling Time Dimensions	16
1.3.5. Modelling Space Dimension	17
1.3.6. Lattice-Based Models	17
2. METHODS	20
2.1. Flux Balance Analysis Scale	22
2.1.1. Genome-Scale Metabolic Networks	22
2.1.2. Flux Balance Analysis	22
2.1.3. Dynamic FBA	23
2.2. Spatial Modelling Scale	24

2.2.1. Boundary Conditions 24
2.2.2. Quorum Sensing Scale 27
2.3. Gene Ontology (GO) Enrichment Analysis 30
3. RESULTS 31
3.1. FBA Results 31
3.1.1. Wild Type Results 31
3.2. One-Species Temporospatial Modelling Results 33
3.2.1. Proliferation of *P. aeruginosa* Across the Space 33
3.2.2. Proliferation of S. aureus Across the Space 42
3.3. Two-Species Temporospatial Modelling Results 44
3.3.1. Proliferation Across the Space 44
3.3.2. Growth on Chronic Wound 46
4. DISCUSSION 51
4.1. Chronic Wounds 51
4.2. Quorum Sensing 52
4.3. Biomass Proliferation and Metabolite Diffusion 52
5. CONCLUSION 53

REFERENCES 54
BIOGRAPHY 65

LIST of ABBREVIATIONS and ACRONYMS

Abbreviation or Acronym		Description
AHL	:	N-acyl homoserine lactones
BC	:	Boundary Conditions
CF	:	Cystic Fibrosis
dFBA	:	Dynamic Flux Balance Analysis
DPD	:	(S)-4,5-dihydroxy-2,3-pentanedione
EPS	:	Extracellular Polymeric Substances
FBA	:	Flux Balance Analysis
GMNs	:	Genome-Scale Metabolic Networks
GPR	:	Gene-protein-reaction
NIH	:	US National Institutes of Health
QS	:	Quorum Sensing
SBML	:	Systems Biology Mark-up Language
XML	:	Extensible Markup Language

LIST of FIGURES

Figure No:		Page
1.1:	Visualization of *P. aeruginosa* biofilm.	2
1.2:	Classes of multi-species biofilm growth.	5
1.3:	Micro-environment of chronic wounds.	9
1.4:	Quorum sensing networks in *P. aeruginosa*.	10
1.5:	Workflow of solving real-world problems with mathematical models.	11
1.6:	Sketch of experimental procedures.	12
1.7:	Genome-scale metabolic networks and material balances.	14
1.8:	Dynamic modelling approaches.	16
1.9:	Types of lattices in lattice-based modelling.	18
1.10:	Biological events and their representations in lattice-based models.	18
1.11:	Physicell, an off-lattice agent-based modelling environment.	19
2.1:	Cyclic representation of the model.	20
2.2:	Discretization of space to the square lattices.	21
2.3:	Illustration of flux balance analysis.	22
2.4:	Boundary Conditions for sourced solid metabolites.	24
2.5:	Regulation laws for reaction boundaries ruled by multiple genes.	25
3.1:	Growth rate change depending on increased PQS release.	28
3.2:	Effect of PQS secretion and glycogen synthase on growth rate.	29
3.3:	Step by step biomass maps taken at certain intervals.	30
3.4:	Biomass growth with and without QS restrictions.	31
3.5:	Step by step biomass maps taken at certain intervals without QS effects.	32
3.6:	Step by step biomass maps taken at certain intervals on a chronic wound	33
3.7:	Portrayal of condition-based biomass growth.	36
3.8:	Gene enrichment analysis.	38
3.9:	*S. aureus* Growth Maps.	43
3.10:	Combined Growth Maps.	44
3.11:	Combined Growth Maps on a Chronic Wound.	46
3.12:	Initial Biomass Location Trials on a Chronic Wound.	48
3.13:	Halved Pyocyanin Impact's effect on the Biomass Map.	49
3.14:	Doubled Pyocyanin Impact's effect on the Biomass Map.	50

LIST of TABLES

Table No:		Page
1.1:	Examples of QS mechanisms for gram-negative bacteria.	7
2.1:	Metabolite Concentrations for *P. aeruginosa*.	25
2.2:	Metabolite Concentrations for *S. aureus*.	26
2.3:	List of Genes that are regulated by Quorum Sensing Mechanism for *P. aeruginosa*.	27
3.1:	Reactions modulated by QS trigger and their respective regulator genes.	31
3.2:	Metabolites accumulated in the environment and uptake rates of the biomass at a specific location for a single iteration after QS is triggered.	39
3.3:	Metabolites not consumed by the model.	39

1. INTRODUCTION

It was well observed for a very long time that bacteria can be hosted by almost any moist surface in nature. They are visible even to the naked eye when adequately thick layer of bacteria is present on the surface and this allows them to be observed even with primitive microscopes. These hospitable surfaces may extend to parts of human body, which may yield malignant outcomes depending on the environment and species involved [1]. Though it was quite observable by many means, it was only after 1980s and 1990s that it was found out that bacteria were living in meticulous ways [2].

1.1. Biofilms

Biofilms are a built-up of microorganisms on phase interfaces, encapsulated in a polymeric matrix. An accumulation of different bacteria within this extra layer of protection may create a well-suited environment for them to proliferate. This guarded environment, while providing housing for growth, greatly boosts their survivability acting as a permeability barrier. While surviving as an individual cell, for example, a unicellular bacterium could be easily washed-out with the fluid stream [3]. Being persistent to fluids within the dense extracellular matrix, which is more formally termed as extracellular polymeric substances (EPS), and having decreased diffusivity in biofilms caused by its hydrophobic quality makes drugs and other external chemicals unable penetrate into it [4]. Hence, when such forms are part of a bacterial infection, antibiotic therapies are not easy stand-alone solutions [5].

By nature, not all biofilms are harmful in effect. As they could adhere to a variety of surfaces including organic as well as inorganic types of surfaces, the hosting may cause biofouling as well as bioremediation. While *Rhodospirillales*, *Sphingomonadales*, and *Rhizobiales* dominate the hazardous side of the community, altering the character of the surface they are attached to in terms of composition or physical attributes [6], there are also useful biofilms. Being able to live in extreme conditions such as high temperature, salinity or pH [7][8] makes some biofilms such as *Desulfitobacterium frappieri* beneficial, used as pesticide and disinfectant [9].

Aside from the habitat, the primary focus of researchers is biofilms forming on organic surfaces as they are affecting the quality of the host's life directly. According

to the US National Institutes of Health (NIH), about 80% of the bacterial infectious disease were caused by structured biofilm communities [10]. Therefore, studying biofilm mechanisms, their formation and structure to reveal how they infect the host and they could be fought against is very important (Figure 1.1) [11]. The most common of such infections are contamination through chronic wounds in diabetic patients in addition to patients after medical device or organ transplantation [12]. Another common area which is prone to infection is the lung [13][14]. Although biofilms are involved in more than 60% of such infections enlisted in medicine, detecting them is difficult in routine diagnostics along as a result of them being well guarded against host defences and antibiotic therapies [15].

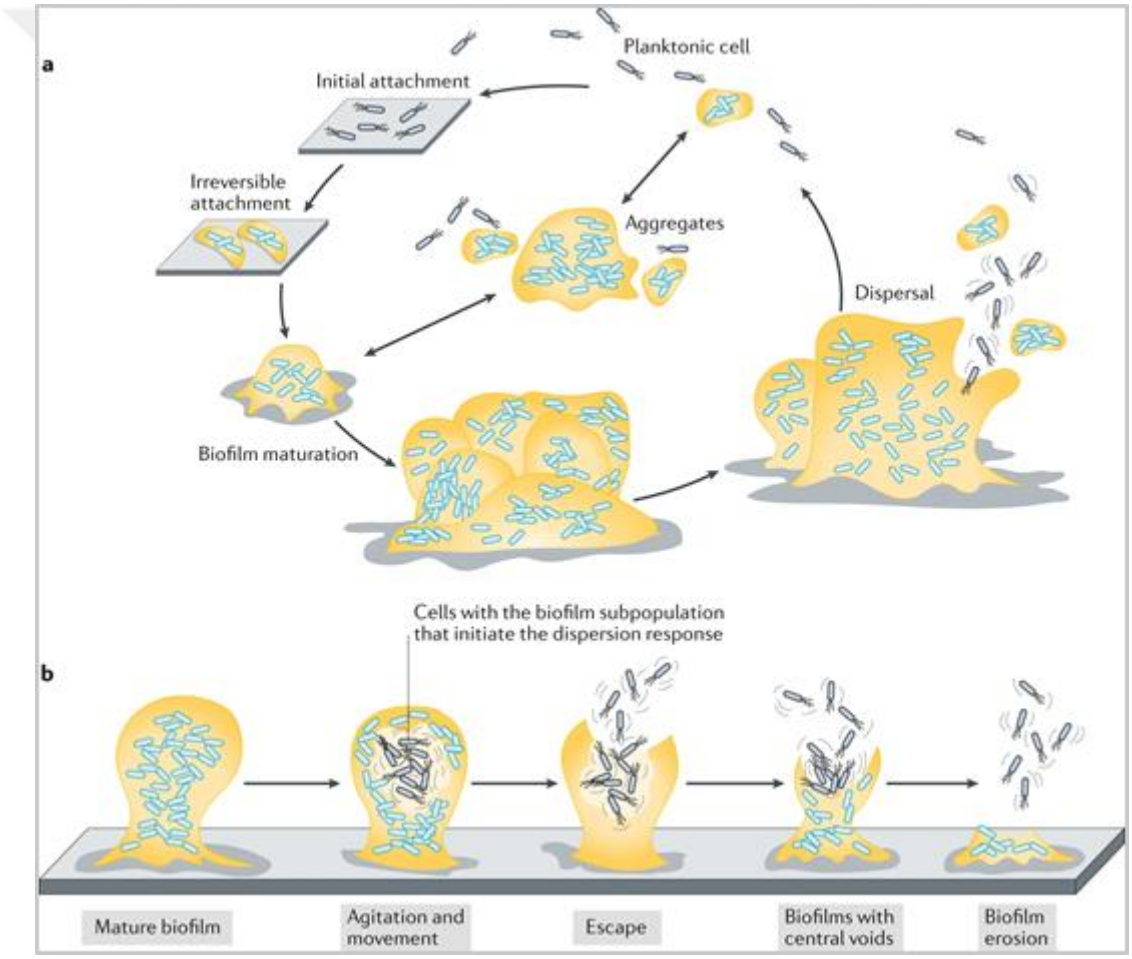

Figure 1.1: a) Phase-based visualization of a single-species *P. aeruginosa* biofilm based on in vitro study. b) Steps of how a mature biofilm disperses.

1.1.1. Biofilm Heterogeneity

Upon taking a closer look, biofilm structure is seen to be a settlement and a factory for a variety of inhabitants. This heterogeneity is categorized under four main parts: Chemical, biological, physical, and geometrical. Distribution across the biofilm is directly linked to these aspects, as the preferences of bacteria differs from one another. The difference in pH, availability of metabolites, substrates, nutrients and their quantity and fluxes etc. plays a role causing a diverse chemical source changing not only from one biofilm to another, but also within the extracellular matrix. This difference in the environment also causes respective population to shift within it creating a biological dissimilarity, more so when secretions and death rate of individual cells are taken into consideration. The density, permeability, viscoelasticity, and viscosity, taken as physical aspects, differs spatially in the biofilm. Lastly, biofilm porosity, thickness, and surface coverage make its structure geometrically unique [16]. Due to these characteristics of heterogeneity, the biofilm cannot be studied as one homogeneous structure, but as a complex system that contains significant levels of variation.

1.1.2. Mono- and Multi-Species Biofilms

Biofilms are classified as mono-species and multi-species depending on the number of species inhabiting their structure. In nature, it is observed that the latter is more redundant compared to the single inhabitant cluster. The many benefits of co-existing, such as metabolic cooperation, co-aggregation, or increased resistance, results in a synergetic life. This synergy could also yield a competitive arena due to metabolic inhibition or competition for metabolites. In general, these interactions occur via quorum sensing (QS) or other metabolic factors [17–19].

Synergetic interactions between species could be categorized in three groups. Firstly, one or more species could cooperate using extracellular metabolites secreted from the other species. *Streptococci* produces lactic acid which is used by *Veillonellae* as a nutrient in the oral biofilm is an example to this interaction also called “syntrophism” [20] [21].

Co-habitation with other species in a microbial community could bring other

benefits. Increased immune or antimicrobial drug resistance is one of the most important aspects that is extensively studied, as drug resistance increases the prevalence of biofilm-related microbial diseases. It has been reported that there are at least three mechanisms that lead to developing resistance [6] [22]. The first mechanism causes drug resistance via the EPS with increased complexity and lowered diffusivity. For instance, a mono-species biofilm of *Staphylococcus epidermidis* develops an EPS significantly easier to diffuse compared to a multi-species biofilm of *Candida albicans* and *S. epidermidis* which may occur after catherer plantation [23].

The second mechanism, although providing no advantage to drug resistance or a protection against the host's immune system, grants favorable environmental conditions for one another to proliferate, e.g. by one of the species consuming relatively toxic materials for the others. An example is a multi-species biofilm of *P. aeruginosa* and *S. aureus* which most commonly observed in lungs as the cause of Cystic Fibrosis (CF). The prior being aerobic, it encapsulates the anaerobic later, acting as a barrier to oxygen penetration in the biofilm while being its sole consumer, resulting in a perfect environment for *S. aureus* growth [24].

The last mechanism is through the expression levels of one or more organisms being affected by the others by means of quorum sensing effects, which may help attain drug resistance. *Streptococcus mutans* and *Veillonella parvula* build a mixed-species biofilm, It has been reported that gene expressions of chlorhexidine, hydrogen peroxide, erythromycin, and zinc chloride related pathways in *V. parvula* differ in mixed-species biofilm, thus provide it with higher resistance when compared to mono-species *V. parvula* [25].

The synergy does not always pose a positive affect. Some species may have antagonistic behavior to others which could be stated under two subgroups. One may outgrow the others in the race for substrates or may directly inhibit their growth. An example to this is a marine biofilm, *Pseudoalteromonas tunicata* which inhibits growth of surrounding microalgea and marine fungi through production of alkyl chain substituents [26]. Not being a biocide and lethal to their targets, synthetic chemicals mimicing these biofilm hamperers are being tested to treat infections [27].

It is vital to understand these interactions as modelling and investigating their behaviour in a given system is inextricable to developing and repurposing drugs.

1.1.3. Spatial Organization of Mixed-Species Biofilm

Not all biofilms are organized in the same way when their spatial formation is inspected. In nature, the living organismsare organized in three different ways: Separate colonization, coaggregation and layering (Figure 1.2) [28].

If there is no mutual relation between two colonies, their micro colonies form in such a way that they barely touch each other, hence they are called separate colonies. [29, 30] Coaggregation, when compared to the other structures, has higher syntrophism as there are two or more species growing together which yields increased metabolic activity and cooperation [30]. Instead of forming separate colonies or sharing a mutual distribution in a rather uniform fashion, one species may "blanket" another and form layers in biofilm [29]. A well-amalgamated and well-layered biofilm is defined by the degree of syntrophy.

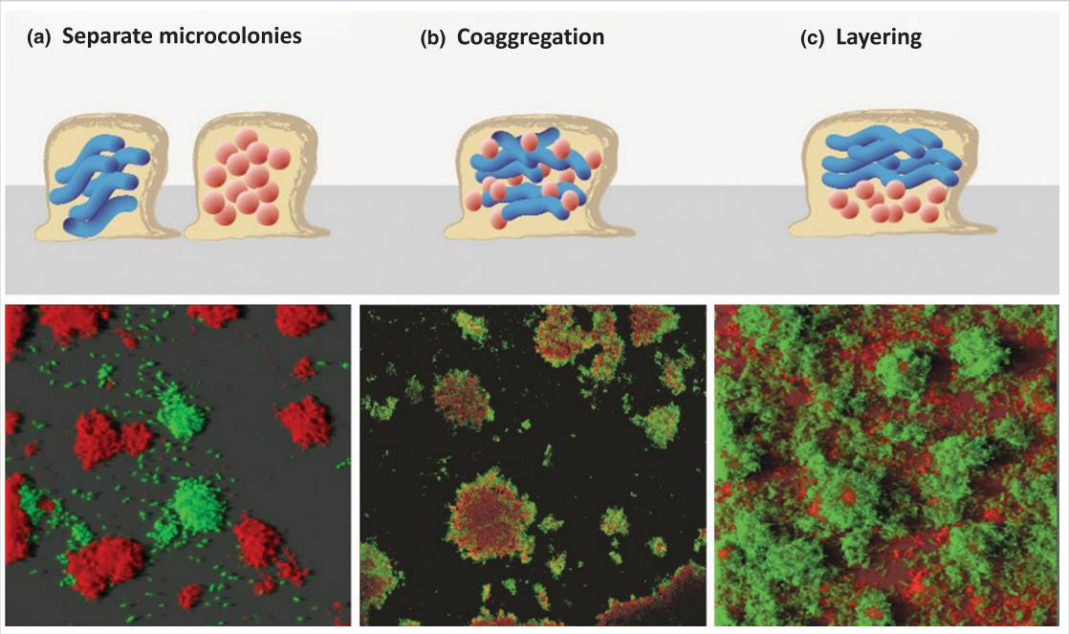

Figure 1.2: Three classes of categorization of multi-species biofilms and their grouping a)Separated colonies, b) coaggregation, c) layering.

How coaggregation occurs in biofilms of mixed species is still an active area of research. An example is the experiment where with *S. gordonii* and *Veillonella atypica* is cultivated in a well-insulated flow-cell system to wash away other planktonic cells to form single species biofilms. Some of these whole biofilms in their early stages were later exposed to each other and their interaction was observed. *S. gordonii* which

were exposed to *V. atypica* had their α-amylase-encoding gene amyB, which raises lactic acid production rate that is a fermentation substrate for *V. atypica*, increased by 20-fold compared to its matured single species biofilm. This effect has been observed to diminish when these films were more than 1 μm away from each other, indicating more research is needed to map the full mechanism [31].

1.1.4. Quorum Sensing (QS)

Communicatication between bacteria, considering a multi-species environment, gives contradictory results when direct links are tried to be drawn as a way of communication on chemical level. To organize the course of action of the group, bacteria secrete extracellular metabolites, generally more than one type, as sensible information according to the organisms to identify the density of the colony or the distance to the source [32]. The cross-talk between cells consists of two features, the first being releasing the signal and the second receiving the message. This phenomenon is known as "Quorum Sensing" (QS). Each bacterial cell produces and then secretes or diffuses a molecule that is named "autoinducer" in low concentration levels. The extracellular metabolites are sensed via bacterial quorum sensing receptors, which leads to the autoinduction of related genes that are regulated by the QS mechanism. Regulated genes could be metabolic, regulatory, or phenotype related [28, 32–34]. An example would be flagella related genes being more active in low autoinducer levels and less active in high QS. In addition, EPS production is increased via the regulated genes while having its growth rate decreased due to high QS [34, 35]. As QS is in a positive feedback loop with genes in charge of autoinducer production, affected bacteria will produce more signal molecules [35].

QS activation and deactivation is regulated by the level of autoinducers. As a certain threshold level has to be exceeded, it is triggered in communities with higher biomass density due to a high concentration of bioinducers. The earliest QS mechanism that has been discovered is in *Vibrio fisher*. As it was part of a gene regulation that is bioluminescent due to excreted material, it was observable by the naked eye when the population grew large enough [36–38]. The next section will have various source and target-specific QS mechanisms explained.

1.1.4.1. Intraspecies QS

When gram-negative bacteria are taken into consideration, N-acyl homoserine lactones (AHL) is the main type of communication, as they bind to R-protein when this group of chemicals given that there is sufficient amount of it available, regulating in their target genes as a result. Various types of these metabolites could be found: 4- to 14- carbon acyl chains with oxo, a hydroxyl or no substitution at their third carbon of the chain [39]. A list of various AHL molecules for spesific gram-negative bacteria and their QS mechanisms is given in the table below (Table 1.1).

Table 1.1: Examples of QS mechanisms for gram-negative bacteria.

Organism	*Major Signal*	*Regulatory Proteins*	*Phenotype*	*References*
Vibrio fischeri	3-Oxo-C6-HSL	LuxI/LuxR	Bioluminescence	[40, 41]
Vibrio harveyi	3-Hydroxy-C4-HSL	LuxLM/LuxN	Bioluminescence	[42–45]
Pseudomonas aeruginosa	3-Oxo-C12-HSL	LasI/LasR	Multiple extracellular enzymes, RhIR,	[46–49]
	C4-HSL	RhII/RhIR	Multiple extracellular enzymes,	[49–52]
Pseudominas aureofaciens	C6-HSL	PhzI/PhzR	Phenazine antibiotics	[53]
Erwinia chrysanthemi	3-Oxo-C6-HSL	Expy/ExpR	Pectate lyases	[54, 55]
Aeromonas salmonicida	C4-HSL	AsaI/AsaR	Extracellular protease	[56]

Acyl homoserine lactones employed by gram-negative bacteria have as their counterpart, oligopeptides, in gram-positive bacteria to mediate communication.

While they employ same chemicals regulating their genes, the reflection on phenotype is not the same for all bacteria. For example, *Bacillus subtilis* and *Streptococcus pneumoniae* use quorum sensing mechanism to increase their biological competence, on the other hand, *Staphylococcus aureus* uses peptides to produce virulence factor while *Enterococcus faecilis* benefits from QS mechanism to regulate conjugation [57–60].

Quorum sensing mechanisms enhance the complexity of modelling biofilms, making it harder to comprehend them thoroughly as the phenotypes of individual cells alters significantly under its effect, which increases further in complexity when changes in autoinducer concentrations and their effects in various levels are considered as an element of the environment.

1.1.4.2. Interspecies QS

As explained in the previous section, each bacterium possesses a unique way of communicating within its population. There is, however, a global autoinducer shared and produced by different species: "Autoinducer-2" (Al-2). Named as interspecies quorum sensing, (S)-4,5-dihydroxy-2,3-pentanedione (DPD) is synthesized by the conserved LuxS enzyme [61]. Ignoring minor differences, this enzyme has been discovered in 35 out of 89 species [62]. AI-2 may induce both inhibition and activation, hence bacteria can either degrade or produce more as needed [61]. DPD is also stated as a possible universal drug target, having different effects on different species, such as its role in virulence factors, biofilm formation, toxin production, or pathogenic cascade on *Shigella, S. gordonii, C. perfringens,* and *V. cholera*, respectively [61, 63, 64].

1.2. Chronic Wounds and Biofilms

A wound is considered chronic when it does not heal within the expected span of healing [65], expected healing time is from four weeks up to 3 months [66]. Diabetes, systemic illness, age, immune suppression, high blood pressure, or infections being among the reasons of the delay, it is estimated that $25 Billion is spent annually solely within the USA on the healthcare cost of non-healing ulcers [67]. The wound,

being open to infections, creates sustained environment for some microbial organisms to proliferate exponentially and produce a more expansionary and invasive biofilm with the contribution of the necrotic tissue and aggregating remains. Comparing acute wounds to chronic wounds, according to a study conducted by the Center for Biofilm Engineering, having a biofilm grown is observed more than ten times as often [12]. Removing the biofilm becomes harder the longer it remains on the wound. Antibiotics developed to treat bacteria fail to penetrate through the biofilm structure, making chronic wound treatment increasingly challenging for medical practitioners [68].

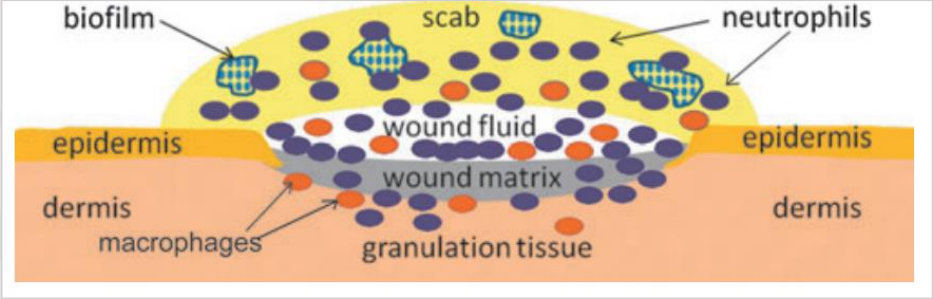

Figure 1.3: Microenvironment of chronic wounds.

Interestingly, biofilms forming over wounds does not settle on the resourceful wound bed but on the scab which prevents the wound from healing (Figure 1.3). The earlier a mature biofilm develops, the harder it becomes for the biofilm to be removed, even an early biofilm of 10 hours may prove nearly impossible to eliminate [69]. Although murine and porcine wound models are developed, it is challenging to deploy them to reflect a chronic wound on humans. Hence, a rational mathematical model should also be developed for humans.

1.2.1. Pseudomonas aeruginosa

Pseudomonas aeruginosa is a gram-negative, aerobic, rod-shaped bacterium that can switch to fermentation which gives it a facultative anaerobic characteristics [70]. Therefore, it is one of the most common causes for nosocomial infectious diseases [71]. Its genome is 5.5-7 Mbp, 65-67% of it being a G + C content, is made up of a single circular chromosome supported by different number of plasmids [72]. When modelling is considered, *P. aeruginosa* provides a sophisticated system. It starts accumulating extracellular material to form its biofilm in a planktonic phase, which

may provide further drug resistance.

Other than the two mechanisms pointed in Table 1.1, LasI and RhlI producing 3-Oxo-C12-HSL and C4-HSL, respectively, 2-heptyl-3-hydroxy-4-quinolone is also used instead of mentioned AHLs as a balance factor between the previous two is shown in Figure 1.4 [71, 73]. It has been shown that silencing the source genes of these autoinducers yields deformed or weakened biofilm structures [74].

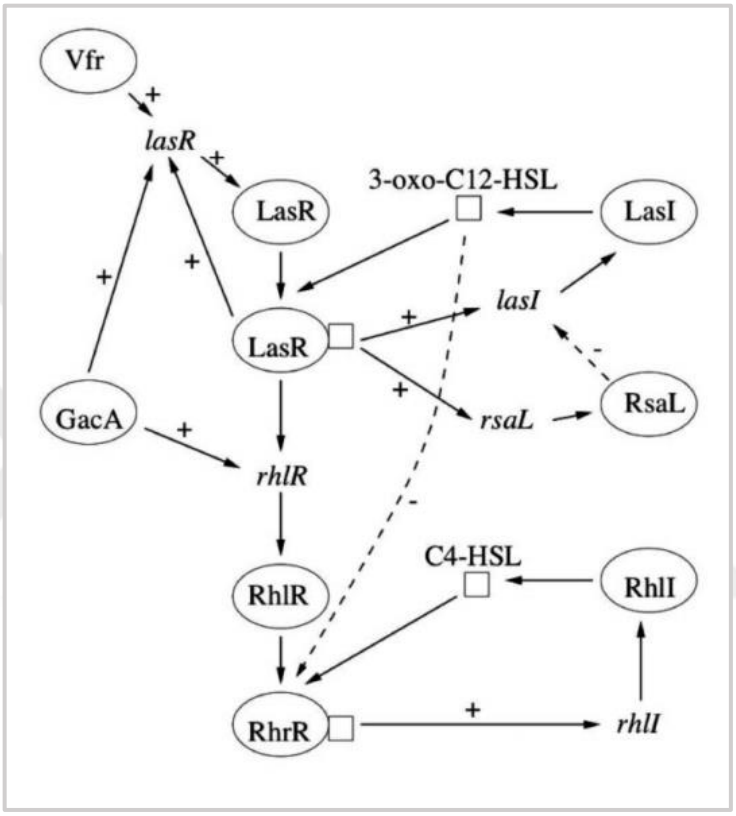

Figure 1.4: Quorum Sensing Networks in *Pseudomonas aeruginosa*.

1.2.2. Staphylococcus aureus

Being part of the human microbiota, Staphylococcus aureus is a gram-positive coccus that under microscope looks like grapes, and it resides mostly on the respiratory tract [75]. Infectious properties are revealed when it is subjected to an environment that contains other bacterial species. It is capable of releasing virulence factors and cause infections, such as skin infections. One of them, staphylococcal scalded skin syndrome could prove fatal for new-born babies [76]. The grapelike structure is the biofilm formed by the bacteria, which provides resistance to drugs. It is even claimed that once a biofilm is formed, *S. aureus* cannot be removed by means of microbial

drugs [77]. Quorum sensing in *S. aureus* community is done by the metabolite named accessory gene regulator (agr). This autoinducer regulates virulence factor, as well as stimulating QS. Although its secretion rate is low, the bacteria entering the body through a vector may attach and construct a biofilm given enough time, hence showing symptoms of infection [78].

1.2.3. Two Species Interaction

A common biofilm found on chronic wounds are combination of *P. aeruginosa* and *S. aureus* communities [79]. Having a mostly mutualistic relationship, *P. aeruginosa* secretes pyocyanin which inhibits *S. aureus* [80]. The integrated biofilm of the two species provides further protection, such as *P. aeruginosa* gaining drug resistance to tobramycin [24].

1.3. Multi-Scale Modelling

Understanding biological systems are cumulative processes which requires consecutive research and experiments. Their outcomes are required to analyse and understand them as a whole. To represent them fully or partially, computational modelling utilizes mathematical terminology and concepts to mirror the process, using numerous variables and expressions to interlink them. Instead of carrying out a full-scale experiment, models may be used to reduce the time of tiresome laboratory work and cost as it could be conducted to give insight about the design before the phase of trial and error. When ethics and impossibility to perform certain experiments are concerned, *in silico* designs serve as a substitute when necessary. Researchers may always convert a question to mathematical realm, solve it, and may try to return to the real solution (Figure 1.5).

To achieve a mathematical solution that would hold as a solution itself, the definition of the problem and its domain is vital. Constructing the domain may be done in different ways such as be discrete or continuous, dynamic or static, deterministic or stochastic, linear or non-linear [81]. As numerous variables and their behaviour must be represented in the model, many different challenges arise when the problem as a model is to be reflected powerfully and sufficiently to avoid under- or over-

representation. Under the concern of inclusivity, researchers should also not ignore the time and power requirement which would result in excessive cost.

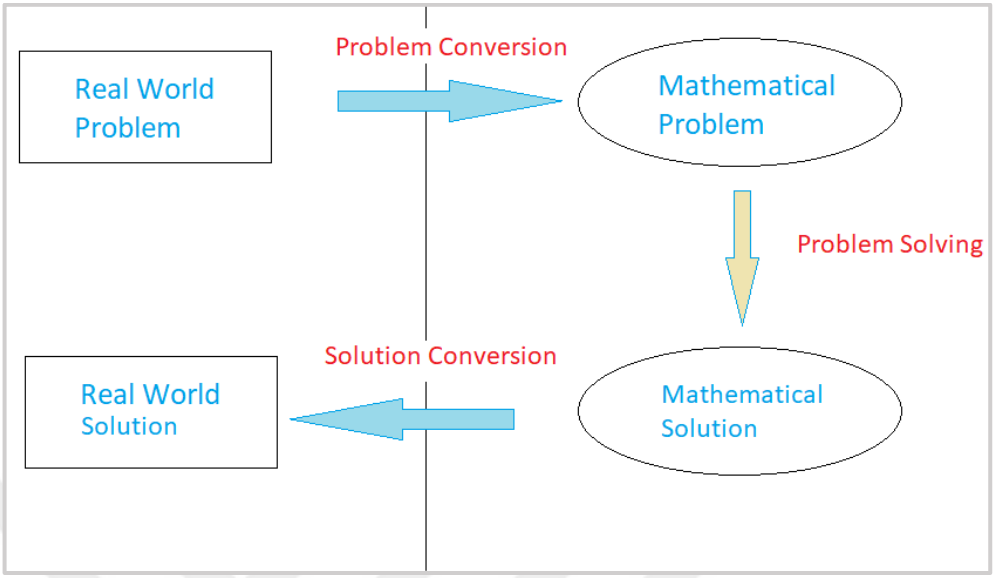

Figure 1.5: Workflow of solving real-world problems with mathematical models.

As the system is converted to a different space, which is a mathematical representation, is bound by the rules of its dimension meaning that its feasibility must be questioned mathematically. Hence, it must be solved accordingly, and the type of solver or the method directly influences the solution derived. Consistent and efficient solutions will require analyses with higher precision and sensitivity and therefore additional computational costs. When a multi-scale model of a biological system is considered, it is mostly conceived as functions of time and space [81, 82], which is a common way to recognize such systems for temporospatial or spatiotemporal modelling. The more complex a system gets the harder it would be to consistently represent the real problem which is also an unignorable concern.

Currently, there are no format universally agreed upon by many multi-scale modelers together, although initial works are to be recognized to make a comprehensive format which could be accepted universally [83].

1.3.1. Systems Biology

Systems biology, being an interdisciplinary field relying on computational methods to enlighten a pre-stated biological question, benefits greatly from high-throughput data to study many interactions, perturbations when necessary to better understand the underlying mechanisms. Therefore, systems biology focuses not merely on discovery but on establishing a structure to utilize the gathered data to perform predictive, hypothesis-oriented science (Figure 1.6) [84].

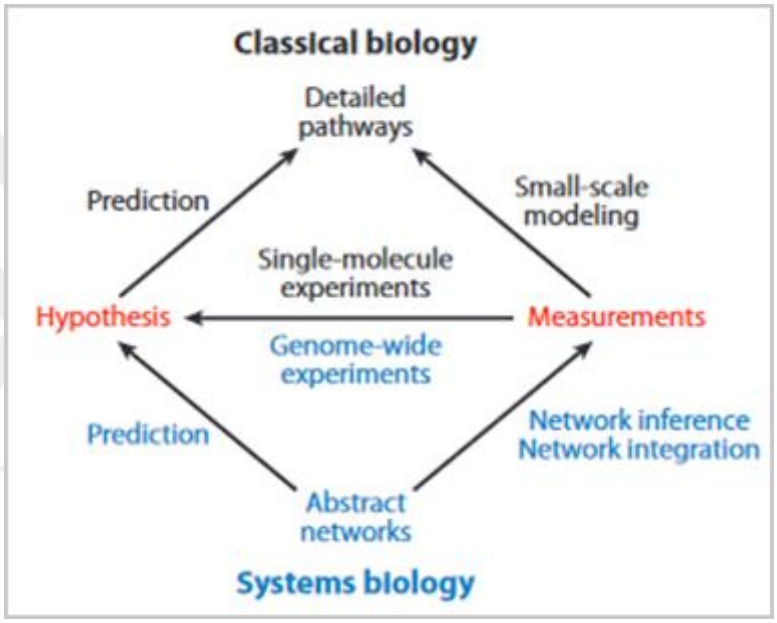

Figure 1.6: Sketch of the experimental procedure in classical biology (top) versus systems biology (bottom).

1.3.2. Genome-Scale Metabolic Networks (GMNs)

Metabolism is a compilation of life-sustaining interactions within a cell. Metabolites are converted into each other in reactions catalysed by thousands of different enzymes, which are proteins translated from mRNAs, carrying information encoded by the related genes. The network of these reactions, reconstructed by systems biology approach, has opened the door for their computational analysis. As a systematic compilation of reactions in an organism, Genome-Scale Metabolic Networks (GMNs) enable us to visualize and analyse individual entities within this large system following the developments in high-throughput data generation

technology in biology. They can be represented by graph-theory as nodes and edges of metabolites and reactions respectively (Figure 1.7a) [85, 86].

Each column representing an interaction, stoichiometry matrices hold information of participating metabolites and their coefficients of the reaction. (Figure 1.7c). ODEs written in a matrix format are than used to calculate reaction fluxes in their presumed steady-state using a constraint-based approach (Figure 1.7c-d).

GMNs are constructed according to gene-protein-reaction (GPR) rules that govern underlying association between reactions and genes via enzymes, and they permit metabolic phenotypes under different conditions to be mimicked by integrating transcriptome data [87]. These enzymes may be encoded by a single gene as well as multiple ones. If more than one of them is involved, they might work both mutually and non-mutually. Considering the structure and function of an enzyme, GPR rules are stated as Boolean logic. It may be controlled by a single gene product, an enzyme complex of multiple subunits, or by isoenzymes.

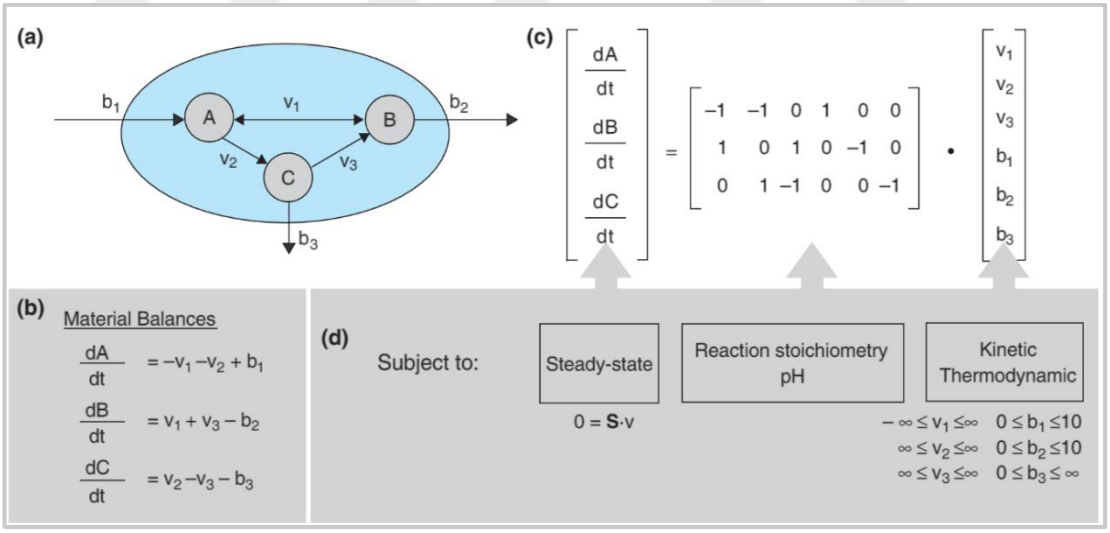

Figure 1.7: Genome-Scale Metabolic Networks and Material Balances a) Toy Model b) Material balances c) Matrix formation from balances at b d) Constraint-based modelling.

A common format to store GMNs is named Systems Biology Mark-up Language (SBML) [88], a type of Extensible Markup Language (XML) format. Having more and more models published, the need of databases and websites that store

them have arisen. BioModels is one such website, which provides access to numerous kinetic or constraint-based mathematical models [89]. It is one of the main sources with almost half of its models already curated. Another source for GMNs is "Virtual Metabolic Human", a website funded by University of Luxembourg, giving access to the human metabolic map which may be navigated under conditions, such as, Parkinson's disease, while containing more than 817 microbiome GMNs [90]. To analyse a GMN in its presumed steady state, constraint-based modelling is the mainstream computational approach (Fig 1.6d). If a model with a dynamic nature is to be constructed, scarcity of kinetic parameters to describe each reaction would be setting a limit as the amount of data required to obtain these parameters create a barrier [36], hence GMN are often analysed under the assumption of steady state. To increase the variety or robustness of the analysis of constraint-based models, algorithms such as GIMME [91], INIT [92], E-flux [93], iMAT [94], or mCADRE [95] provides support to integrate transcriptomics data with GMNs.

1.3.3. Modelling Approaches

According to the scope of a biological phenomenon, multi-scale models are built considering the system levels. An example of a lower-level biological question might be on proteomic level, such as protein-protein interactions or signalling, while a high-level scale may be between different cell types within a tissue or an organ. Depending on this scale, modelling approach is commonly divided into two groups: Top-down and bottom-up. Depending on the data available and their respective advantages and disadvantages, along with level of the scale, determining which approach to use is vital.

Beginning with the fine details of information and building from it, the intent of a bottom-up approach is to achieve a global model, intertwining all accumulated information. Therefore, molecular interactions are vital, and the data collected is to be piled-up, starting from a lower level. [93]. In addition to having the model consider each cell and their interactions in entirety, it brings the flexibility to alter the details to check their individual outcomes. As in this instance, each mechanism that is represented in the GMN of the bacterium may be tweaked separately to look for plausible solutions, giving the ability to gather fine details without much complication,

In addition, this welcomed complexity may bring high computational needs, increasing the cost, although this has not hindered people from attaining valuable models [81, 96].

1.3.4. Modelling Time Dimensions

In both ODEs and PDEs, time is taken as the independent variable as a biological system revolves around its change, as the change of the biological profiles between two points of it gives the dynamics of the profiles desired to be studied. There are two approaches to appraise this change in time in the models: Discrete and continuous.

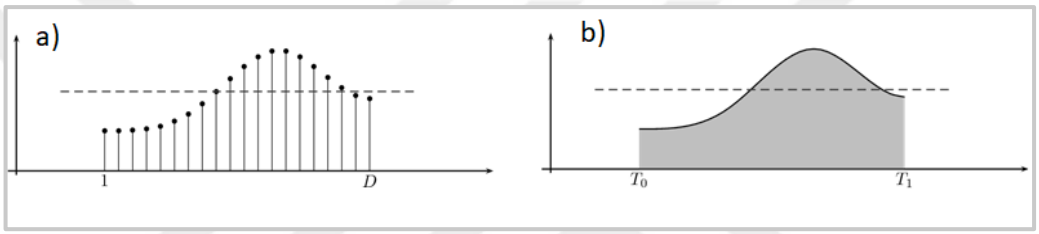

Figure 1.8: Dynamic modelling approaches a) Discrete b) Continuous.

1.3.4.1. Discrete Time

When a given interval of time could not be conveyed in continuous time, such as a Boolean model which is built as difference equations (Boolean functions), it is required to divide the interval in equal parts of time points, which are then taken as iterations to be calculated according to stated equations [97, 98]. Being presumed as in quasi-steady state, constraint-based metabolic models are not prone to be stated in continuous time dimensions. As from numerous to an enormous number of components are modelled at once, in the sense of simplicity of calculations, favouring discrete time instead of its continuous counterpart is more acceptable as it curbs the number of time points (Figure 1.8a).

1.3.4.2. Continuous Time

Kinetic models, stated as a system of ODEs or PDEs, are studied in non-discretized time, as they are continuous functions of it (Figure 1.8b). Solving these

systems with respect to time requires computational power, when the given system is large enough. There are a number of solvers available on different software or programming languages, such as MATLAB, COPASI or Python, still, it is fundamental to choose a specific type of solver if the stiffness of the problem is a concern [99]. With the power of computational analysis, the distance between each point of intervals is minimized. Hence, the assumption of continuity is accepted, ignoring the fact that these solvers still function by discretising the time. If not kinetic but stochastic modelling is desired, appropriate solvers are available in most software.

1.3.5. Modelling Space Dimension

Just as time dimension, space dimension could also be perceived as discrete and continuous. Space can be dissected, making it discretized in parts called a lattice, although the name is not approach specific, as it is used for continuous spaces. In the following part, both types of lattices are defined and depicted using the same subjects.

1.3.6. Lattice-Based Models

Lattices, which are framed on pre-determined volumes of discrete spaces, may come in different geometric shapes. The size may be subject to change depending on outside effects, such as pull and push response or density (Figure 1.9c). If a dynamic lattice is being modelled to better reflect the phenomena, the complexity arising would greatly increase the computational cost, while returning detail and coherence.

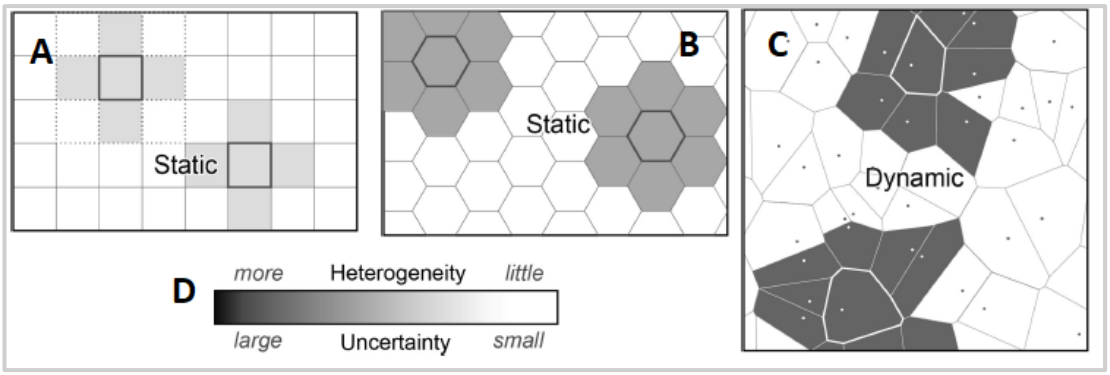

Figure 1.9: Types of lattices in lattice-based modelling A) Square B) Hexagonal C) Dynamic.

As information may be stored in lattice-based space, any detail about a biological system and its change may be depicted. A good example would be migration, individual or quantified biological bodies moving to adjacent spaces as in proliferation (Figure 1.9a). Although a single slice of a lattice could be presumed to store only one biological entity (cellular automata or Ising model), a single body could as well reside on more than one piece of those spaces, which is named as Cellular-Potts model [100–102]. To establish a multiscale biological systems model, there are also specific lattice-based modelling software [103–105].

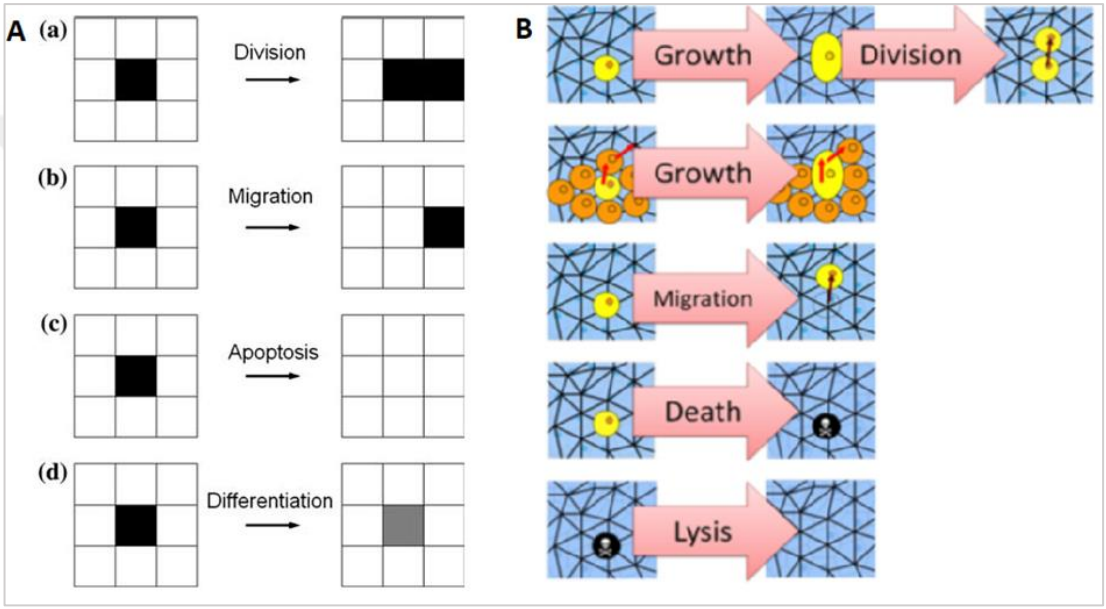

Figure 1.10: Biological events and how they are represented in lattice-based models A) Square Lattice B) Lattice-based agent modelling.

Another lattice-based method is agent-based modelling. In this method, each and every cell act as a ‘agent’ migrating through the meshed lattice. Phenotype of these sole cells are subject to biological phenomena across the lattice, such as pulling or pushing, attachment, expansion, and bonding, while the rest of the basic events occur. As an example to such software, BacArena is one of the pioneers for modelling microbial communities metabolically [106].

1.3.6.1. Off-Lattice Models

Taking the space as a continuous entity, off-lattice method demands high level computational power to derive coherent results. PhysiCell is among software capable of establishing and simulating multi-scale off-lattice models through BioFVM, developed by the team, which initiated as a spatial diffusion physics motor (Figure 1.11) [107, 108]. Lacking constraints, agents may be set to be freely accessible anywhere in space, while metabolites and other chemicals diffuse in respect to Fick's diffusion law.

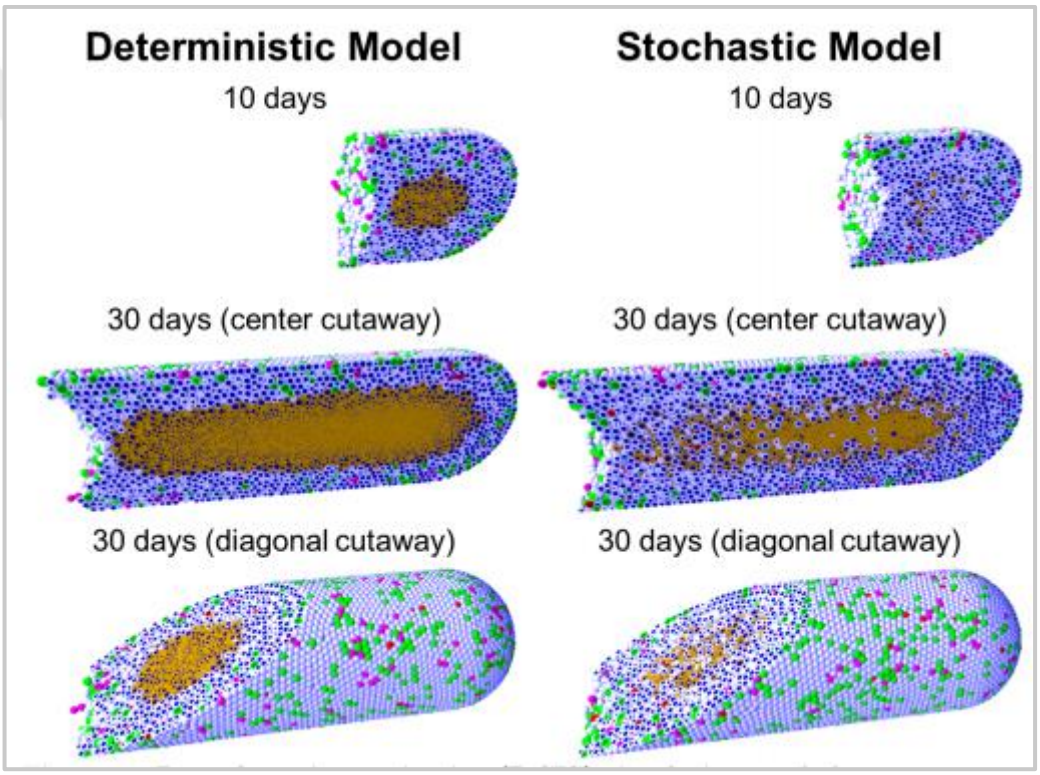

Figure 1.11: PhysiCell is an off-lattice agent-based modelling environment.

2. METHODS

The temporospatial model is a three-phased model, each following one another to create a dynamic, living environment where the bacterium grows. The first step updates the environment, based on the available constraints, diffused from the nutrient-available boundary of the lattice, taking diffusion constants into consideration, up to where biomass is present. This new environment profile is then used to determine upper and lower boundaries of the model for each individual compartment of the lattice. As diffusion into a biofilm, after the QS effects are triggered, would be lower in numbers due to the bacteria being trapped in the EPS. As the second step, growth rates of biomasses in compartments as well as their production/consumption rates (fluxes) are calculated via Flux Balance Analysis, followed by the deduction of consumed metabolites through exchange reactions from the environment. The third step is the proliferation of biomasses after growth. The new biomasses migrate to adjacent lattices according to the species-specific diffusion coefficient. After the cycle is complete, a new iteration starts to repeat the cycle, creating a growth model of bacterium (Figure 2.1).

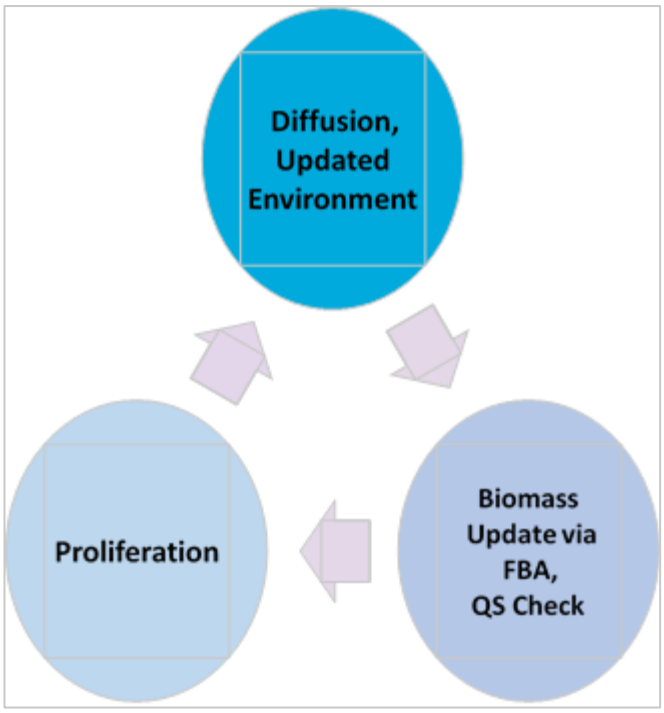

Figure 2.1: Cyclic representation of the model.

As the space is designed as a lattice, each compartment stores its own profile for biomasses and extracellular metabolites separately, which allows the FBA phase of the model to be performed respectively. Each iteration of FBA gives an updated measure of biological bodies (Figure 2.2). Values of diffusion constants taken from the literature are used to calculate availability of each metabolite, which are 0.0003 cm^2s^{-1} for the bacterial movement, and 6.4 x 10^{-6} cm^2s^{-1} for all metabolites based on diffusion rate of glucose [109, 110].

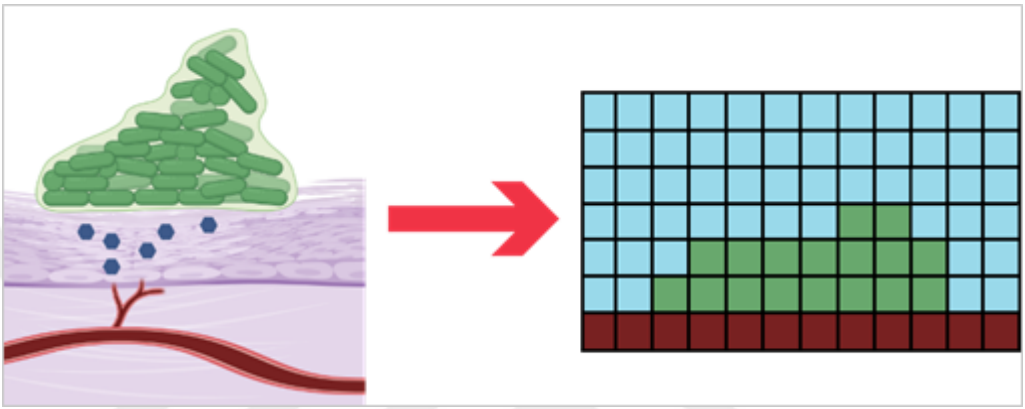

Figure 2.2: Discretization of space to the square lattices.

P. aeruginosa is known to secrete pyocyanin which inhibits and lyse *S. aureus* and other bacteria [80]. In addition to the death rate of *S. aureus*, which is set to 0.2 for both bacteria, an additional 0.4 multiplier is used which is taken from a similar work [96], adjusted according to *P.* aeruginosa biomass, resulting the Equation 1.1:.

$$Dr_{sa} = 1 - ((1-0.2) - (0.2*0.4 * (B_{pa}/ B_{total}))) \quad (1.1)$$

where Dr_{sa} is the death rate of *S. aureus*, B_{pa} is the biomass of *P. aeruginosa* in the given grid and B_{total} is the total biomass in the grid.

2.1. Flux Balance Analysis Scale

2.1.1. Genome-Scale Metabolic Networks

Genome-Scale Metabolic Network 'PAO1' of *P. aeruginosa*, is downloaded from BioModels numbered as MODEL1507180020 in XML format. There are 1054 genes, 879 metabolites and 1110 reactions in the model, 121 of which are exchange reactions. The model yields consistent and plausible results compared to aerobic glucose experiments[111]. *S. aureus* model is also downloaded from BioModels numbered as MODEL1507180072 in XML format. There are 801 metabolites and 860 reactions in the model, 87 of which are exchange reactions [112]. To analyse the models, they are deployed in Python via CobraPy package [113], which is one of the most inclusive constraint-based analysis tools.

2.1.2. Flux Balance Analysis

It is both impractical and almost impossible to measure every single reaction rate in a given cell. Accepting each cell being in its quasi-steady state, Flux Balance Analysis is objectified to find the unknown fluxes by coursing through the optimal solution for a pre-determined set of objective function and constraints (Figure 2.3) [114]. As linear programming generates consistent results, measured uptake rates of chemicals can be conveyed to reduce the number of unknown fluxes, which results in a more realistic solution [114].

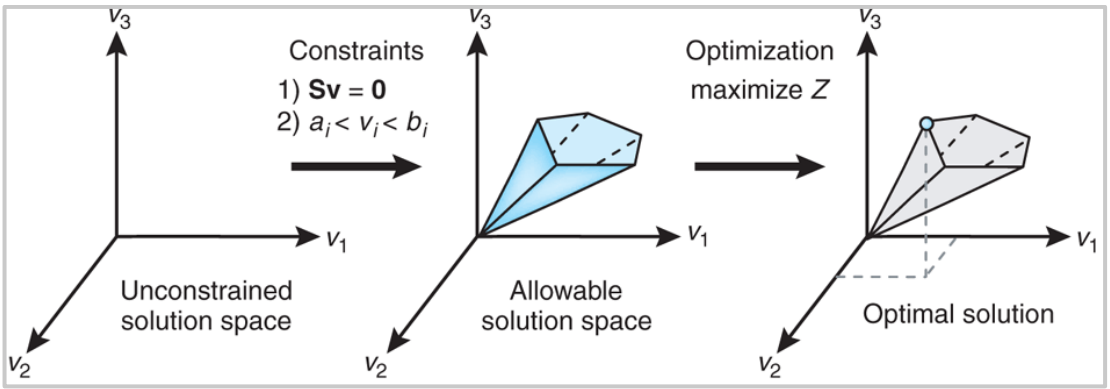

Figure 2.3: Flux Balance Analysis Optimization.

FBA is easily represented as a linear optimization problem. As the solver of this linear problem, the optimization is performed by Gurobi Optimization Solver integrated into CobraPy, which is available for academic purposes for free.

2.1.3. Dynamic FBA

Considering time points of discrete intervals, performing an FBA for each consecutive step results in dynamic chain of events. Dynamic Flux Balance Analysis (dFBA) aims to derive such behaviour of metabolic models. As each step is considered a separate steady state following an FBA, consumption and production of metabolites could be calculated respectively according to fluxes calculated.

$$Substrate\ Available = \frac{S_c}{X \cdot \Delta t} \tag{2.1}$$

Metabolite and biomass concentrations are derived using the Equation 2.1 to determine conditions for the following FBA step. S_c , X and Δt stand for substrate concentration, biomass concentration and time interval, respectively.

$$\frac{dX}{dt} = \mu X \ \rightarrow X = X_o \cdot e^{\mu \Delta t} \tag{2.2}$$

$$\frac{\partial S_c}{\partial t} = -S_u \cdot X \ \rightarrow S_c = S_{co} + \frac{S_u}{\mu} X_o (1 - e^{\mu \Delta t}) \tag{2.3}$$

Stating the change in biomass as an ODE, the final quantity of biomass can be derived using the growth rate directly obtained from FBA results. Then, concentrations of extracellular metabolites can be calculated according to Equation 2.3. To be able to perform this calculation, initial concentration of both biomass and metabolites are required. Although the concentration available could be calculated in each FBA using the last equation, it is chosen that an exhaustive approach in terms of metabolites available as ignoring the possibility that not an entirety of a metabolite available would come in contact with the organism, which means that if a metabolite is present in a grid of the lattice, it can be consumed fully.

In the combined model of two-species, available extracellular metabolites are

divided between the species according to their biomass levels compared to the total biomass in a compartment.

2.2. Spatial Modelling Scale

The approach of the temporospatial modelling in this study is lattice-based which means that partial differential diffusion equations (Fick's Law) used in this study must also be mapped to discrete space, also required for the programming aspect. To do that, a finite difference method is applied. Step by step method is shown below.

$$\frac{\partial U}{\partial t} = D\left(\frac{\partial^2 u}{\partial x^2} + \frac{\partial^2 u}{\partial y^2}\right) \tag{2.4}$$

$$\frac{u_{i,j}^{(n+1)} - u_{i,j}^{(n)}}{\Delta t} = +D\left[\frac{u_{i+1,j}^{(n)} - 2u_{i,j}^{(n)} + u_{i-1,j}^{(n)}}{(\Delta x)^2} + \frac{u_{i,j+1}^{(n)} - 2u_{i,j}^{(n)} + u_{i,j-1}^{(n)}}{(\Delta y)^2}\right] \tag{2.5}$$

$$u_{i,j}^{(n+1)} = u_{i,j}^{(n)} + D\Delta t\left[\frac{u_{i+1,j}^{(n)} - 2u_{i,j}^{(n)} + u_{i-1,j}^{(n)}}{(\Delta x)^2} + \frac{u_{i,j+1}^{(n)} - 2u_{i,j}^{(n)} + u_{i,j-1}^{(n)}}{(\Delta y)^2}\right] \tag{2.6}$$

2.2.1. Boundary Conditions

To determine chemical concentrations in each compartment after diffusion, Eq(2.6) is used with specific diffusion constants. As solid metabolites would be unable to diffuse without direct contact to the biofilm or an area inhabited with bacterium, any grid containing metabolites are therefore set as zero.

Depending on the metabolite, the boundary conditions (BC) of the system differs. While Neuman boundary conditions confine the values of metabolites within the entirety of the lattice, preserving total sum of metabolites, Dirichlet boundary conditions directly source the system with metabolites. Values for the concentration of each metabolite available in blood plasma on a given scar on the human skin is taken from "The Human Metabolome Database" listed in Table 2.1-2.2 [115]. The data is rearranged manually, taking the average of the data available of healthy cases according to the exchange reactions present in the model, as there are many condition-specific measurements, and means of values are taken as the initial concentration.

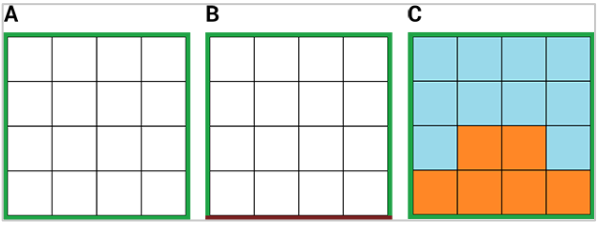

Figure 2.4. Boundary Conditions for sourced solid metabolites A) Solid Metabolites Not Sourced, B) Solid Sourced Metabolites from wound C) Oxygen (Green is Neuman BC, Red is Dirichlet BC).

If the source of a solid metabolite is solely the biofilm itself, only Neuman type BCs are necessarily applied, which means that there would be no leakage from the system. However, metabolites sourced from the boundary of the lattice are diffused according to Dirichlet BCs (Figure 2.4). As oxygen is sourced from any location lacking biomass, the system is rich in terms of oxygen. Migration of biomass is also implemented by using Equation (2.6), which is widely used in literature [116].

Table 2.1:. Extracellular Metabolite Concentrations for *P. aeruginosa* (mmol/L).

Metabolite	**Uptake**	**Metabolite**	**Uptake**	**Metabolite**	**Uptake**
2dhglcn	0	g15lac	0.048	na1	0.025
4abut	0.0005	gbbtn	0.0015	nh4	0
4hbz	0.0024	gcald	0	ni2	14
5mta	0	glc	0	no2	0.127
PA_LPS_A	0	glcn__D	0	no3	0.0006
abtn	0	gln__L	5.4	o2	0.032
ac	0.0419	glu__D	0.0033	ocdca	0.0418
acald	0.001	glu__L	0.6579	ohexa	6.96
ad	0.0006	glutar	0.0001	orn__L	0.4675
agm	0	gly	0.0652	orot	0
akg	0.0089	glyb	0.0008	palmACP	0.0938
ala__B	0.003	glyc	0.3299	pepd	0.005
ala__D	0.4446	glyc3p	0.082	phe__L	0
ala__L	0.4272	gua	0.053	pi	0
algna	0	h	0.03	ppn	0.057
alltn	0.0021	h2o	0	pqs	0.8204
arg__L	0.1295	hdca	55000	pro__L	1.285
ascb	0.0608	hexs	0	prolb	0
asn__L	0.0329	his__L	1.0646	ptrc	0.1983
asp__L	0	hxan	0	pyr	0.01
btd__RR	0	ile__L	0.08	rib__D	0.0001
buts	0	k	0.011	ser__D	0.063
cd2	0	lac__L	0.0775	ser__L	0.0023

Table 2.1: Continued.

Metabolite	Uptake	Metabolite	Uptake	Metabolite	Uptake
cellb	0	leu__L	4.2	so4	0.0023
chol	0.0145	lys__L	1.51	spmd	0.1598
cit	0	mal__D	0.16	succ	0.49
co2	26	mal__L	0.198	taur	0.0103
cobalt2	0	maln	0	thm	0.0235
crn	0.043	man	0.012	thr__L	0.162
csn	0.0064	met__D	0.015	ths	0.0001
cu2	0.017	met__L	0.064	toh	0.1277
cys__L	0.212	mg2	0	tr	0
cyst	0.109	mn2	0.0334	trp__L	0.0784
dad__5	0	mnl	0.833	tyr__L	0.072
fe2	0	mobd	0.0002	ura	0.0021
fe3	0.04	mso3	0.034	urea	4.53
feenter	9.766	muc	0	val__L	0.233
ferrich	0.0167	myrsACP	0	xan	0.0007
fmet	0	myrt	0	xyl__D	2.4431
fru	0	n2	0	zn2	0.0135
fum	0				

Table 2.2: Extracellular Metabolite Concentrations for *S. aureus* (mmol/L).

Metabolite	Uptake	Metabolite	Uptake
EX_Isomaltose_e	0.0	EX_L__Leucine_e	0.16
EX_H_e	0.0	EX_L__Lysine_e	0.198
EX__LPAREN_R_RPAR___Lac_e	1.51	EX_L__Proline_e	0.1983
EX__LPAREN_S_RPAR___Lac_e	0.0	EX_L__Valine_e	0.233
EX__LPAREN_S_RPAR___Mal_e	0.012	EX_Maltodextrin_e	0.0
EX_Na_e	14.0	EX_Melibiose_e	0.0
EX_2__Oxoglutarate_e	0.0089	EX_Mn2_e	0.0002
EX_Acetate_e	0.0419	EX_Molybdate_e	0.0
EX_Alkylphosphonate_e	0.0	EX_NH3_e	0.035
EX_alpha__Methyl_glutamate_e	0.0	EX_Ni2_e	0.0006
EX_Antimonite_e	0.0	EX_Nicotinamide_e	0.0
EX_Arsenite_e	0.0	EX_Nicotinate_e	0.0
EX_K_e	4.2	EX_Nitrate_e	0.0418
EX_Carnitine_e	0.043	EX_Nitrite_e	0.032
EX_Choline_e	0.0145	EX_Orthophosphate_e	1.285
EX_Mg2_e	0.833	EX_Oxygen_e	6.96
EX_CO2_e	26.0	EX_alpha__Trehalose_e	0.0
EX_Cobalt_e	0.0	EX_Arbutin_e	0.0
EX_D__Alanine_e	0.4446	EX_D__Fructose_e	0.048
EX_D__Fructose_6__phosphate_e	0.0102	EX_D__Glucose_e	5.4
EX_D__Galactose_6__phosphate_e	0.0	EX_D__Glucoside_e	0.0
EX_D__Gluconic_acid_e	0.0	EX_D__Mannitol_e	0.034
EX_D__Glucose_1__phosphate_e	0.0	EX_D__Mannose_e	0.064
EX_D__Glucose_6__phosphate_e	0.0291	EX_Lactose_e	0.0
EX_D__Glutamate_e	0.0001	EX_Maltose_e	0.0

Table 2.2: Continued.

Metabolite	Uptake	Metabolite	Uptake
EX_D__Mannose_6__phosphate_e	0.0	EX_N__Acetyl__D__glucogen_e	0.0
EX_D__Ribose_e	0.0023	EX_Phosphonate_e	0.0
EX_D__Serine_e	0.0023	EX_Putrescine_e	0.0001
EX_D__Tagatose_6__phosphate_e	0.0	EX_Pyrimidine_e	0.0
EX_Ethanol_e	0.04	EX_Raffinose_e	0.0048
EX_Fe3__ferrichrome_e	0.0167	EX_Sorbose_1__phosphate_e	0.0
EX_Glycerol_e	0.053	EX_Spermidine_e	0.0103
EX_Glycine_e	0.3299	EX_Sucrose_e	0.0018
EX_Glycolate_e	0.0079	EX_Sulfide_e	0.0
EX_sn__Glycerol_3__phosphate_e	0.03	EX_Sulfite_e	0.0
EX_H2O_e	55000.0	EX_Sulfur_e	0.0
EX_Hg2_e	0.0	EX_Teichoic_acid_e	0.0
EX_Iron_e	9.766	EX_Thiamin_e	0.0001
EX_L__Alanine_e	0.4272	EX_Thiosulfate_e	0.0
EX_L__Arginine_e	0.1295	EX_Uracil_e	0.0021
EX_L__Ornithine_e	0.0938	EX_Ascorbate_e	0.0608
EX_L__Glutamate_e	0.0652	EX_Xanthine_e	0.0007
EX_L__Glutamine_e	0.6579	EX_Zn2_e	0.0135
EX_L__Isoleucine_e	0.0775		

2.2.2. Quorum Sensing Scale

Instead of a slow and steady build-up of QS signals, the system is working with a simple switch of “no-QS” to “QS”, which can be interpreted as the bacterium is already trapped in biofilm in the given lattice. The switch is turned on depending on the amount of biomass accumulated, the threshold being set as 15 (g dry weight (mmol Glc)$^{-1}$).

Linked to the expression levels of genes, their related reaction’s lower boundary is altered accordingly. If a gene is downregulated, the aforementioned boundaries are expected to decrease. Similarly, if they were to be upregulated, their boundaries are expected to increase which applies to genes affected by QS mechanisms, respectively. In addition to directly affiliated genes, additional genes may be involved in ruling of a certain reaction, so a logical representation is needed for its control. Assuming that gene “A” is regulated by QS mechanisms, and gene “B” being a gene not disrupted by such changes, there are four possible cases (Figure 2.5). Given that “A” is downregulated or upregulated, if they both govern the same reaction together, there would be no changes for boundaries of the related reaction. If either of the genes regulate the reaction, as in an “OR” relationship, boundaries increase or decrease, respectively, considering that lower bounds are negative numbers in models.

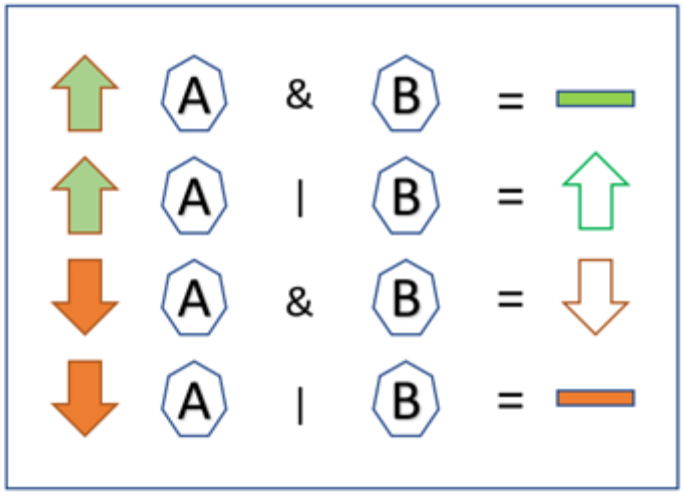

Figure: 2.5: Regulation laws for reaction boundaries ruled by multiple genes.

In PAO1 *P. aeruginosa* model, autoinducer PQS is among the exchange reactions listed, which may allow one of the QS regulations to be modelled. The mechanism controls 19 genes through 8 metabolic pathways in the bacteria, some of which are listed below (Table 2.1.).

Table 2.3: List of Genes that are regulated by Quorum Sensing Mechanism in *P. aeruginosa* metabolism.

Description	**Locus Tag**	**Gene**	**Fold Change**	**Reference**
Glucose metabolism				
Glucose-6-phosphate 1 dehydrogenase	PA3183	Zwf	Up	[117]
Phosphogluconate dehydratase	PA3194	Edd	Up	[117]
2-Ketodeoxyphophogluconate aldolase	PA3181		Up	[117]
Electron transport and oxidative phosphorylation				
Nitrate reductase subunits	PA3872-3875	narlJHG	Down	[118]
Acetate metabolism				
Acetate-CoA ligase	PA0887	acsA	Down	[117]

Table 2.3: Continued.

Description	Locus Tag	Gene	Fold Change	Reference
Activated methyl cycle				
5-Methyltetrahydropteroyltriglutamate-homocysteine S-methyltransferase	PA1927	metE	Up	[118]
Tyrosine degradation				
Maleylacetoacetate isomerase	PA2007	maiA	Down	[117]
Fumarylacetoacetase	PA2008	fahA	Down	[117]
Homogentisate 1,2-dioxygenase	PA2009	hmgA	Down	[117]
Tryptophan degradation				
Anthranilate dioxygenase reductase	PA2514	antC	Up	[117]
Anthranilate 1,2-dioxygenase subunit beta	PA2513	antB	Up	[117]
Anthranilate 1,2-dioxygenase subunit alpha	PA2512	antA	Up	[117]
Rhamnolipid biosynthesis				
Rhamnosyltransferase 1 subunit A	PA3479	rhlA	Up	[117]
Rhamnosyltransferase 1 subunit B	PA3478	rhlB	Up	[117]
Rhamnosyltransferase 2	PA1130	rhlC	Up	[117]
Glycogen biosynthesis				
Glycogen synthase	PA2165		Up	[117]

2.3. Gene Ontology (GO) Enrichment Analysis

As molecular biology has increasingly become a data-intensive discipline, ontologies have emerged as an essential computational tool to assist in the organisation, description and analysis of data. Ontologies describe and classify the entities of interest in a scientific domain in a computationally accessible fashion such that algorithms and tools can be developed around them. The technology that underlies ontologies has its roots in logic-based artificial intelligence, allowing for sophisticated automated inference and error detection.

In order to comprehend gene functions, an inclusive database assembled by structured vocabularies (ontologies) named Gene Ontology (GO) is built to provide vital information to describe and classify genes, giving access to their biological process, molecular function and cellular components [119]. To analyse genes regulating reactions that are affected by QS mechanisms, PANTHER (Protein ANnotation THrough Evolutionary Relationships), a comprehensive classification system that includes gene function ontology, pathways and statistical analysis tool [120] is used through “geneontology.org” web-based tool [119].

3. RESULTS

3.1. FBA Results

3.1.1. Wild Type Results

P. aeruginosa is an aerobic, gram-negative bacteria and it uses glucose as one of the main carbon sources as any other bacterium, hence glucose availability is the main factor effecting growth rates. The model "PAO1 iMO1056" is mathematically analysed to obtain coherent wild-type results. CobraPy is used to do the reading of the biological model in Python and the optimization of functions is done with the support of Gurobi optimization using CobraPy. The resulting biomass growth rate which is the objective function of the optimization to maximize is yielded as 1.0479 h^{-1} on par with published outcomes [111] which results in 0.10479 g dry weight x (mmol Glc) $^{-1}$ of biomass as the result of FBA, yielding the exact number provided by the developers of the model.

S. aureus model, on the other hand, had no validation carried out for its GMN, and had all its exchange boundaries set to either -10 and 10 for lower and upper bounds. As a result, a basic validation was carried out in this study using provided metabolites in Table (2.2) and comparing the doubling time to the literature.

3.1.1.1. PQS Secretion Reaction of *P. aeruginosa*

When the model is investigated, PQS is found to be the major metabolite for quorum sensing analysis, hence it was the focus for a specific metabolic driven approach. PQS production has a positive feedback mechanism, and its regulation depends on the autoinducer level present in the given environment.

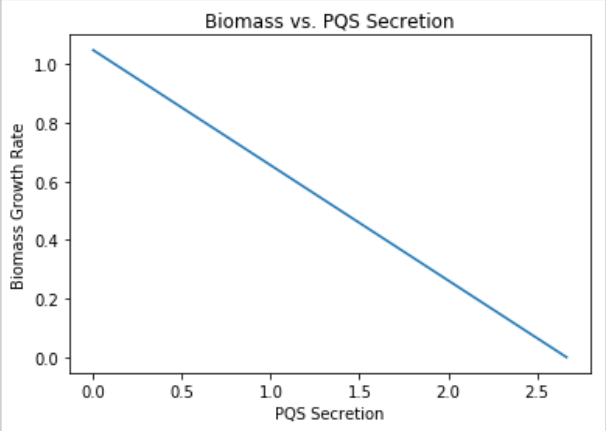

Figure 3.1: Growth rate change depending on increased PQS release.

As the model is forced to secrete more PQS, the biomass growth rate decreases respectively as seen in Figure 3.1. This is on par with the information found in the literature regarding QS mechanism which effects the metabolism directly [121]. A hand-picked PQS secretion quantity which would not diverge considerably from results available in the literature would be 0.15 as a lower boundary and a possible 0.75 for a high-QS situation, resulting in 0.989 and 0.7532 growth rates respectively. As an approximation to in vitro findings, the QS mechanism trigger is set such that the uptake rates would be lowered to a quarter of the diffusion occurring when no biofilm is present, as biofilm permeability and diffusibility would be lowered as biofilm formation progresses [122].

3.1.1.2. Glycogen Synthase, PQS Secretion and Growth Rate Relationship

In addition to PQS secretion being the intermediate for communication across bacterium, glycogen synthesis should be investigated as its accumulation within the cell is required for biofilm accumulation [123]. The relationship between biomass, PQS and glycogen production rates can be seen in Figure 3.2. The graph leaning towards the PQS secretion axis means that the model is more sensitive to changes in PQS boundaries rather than the boundaries of glycogen synthesis, while reducing the growth.

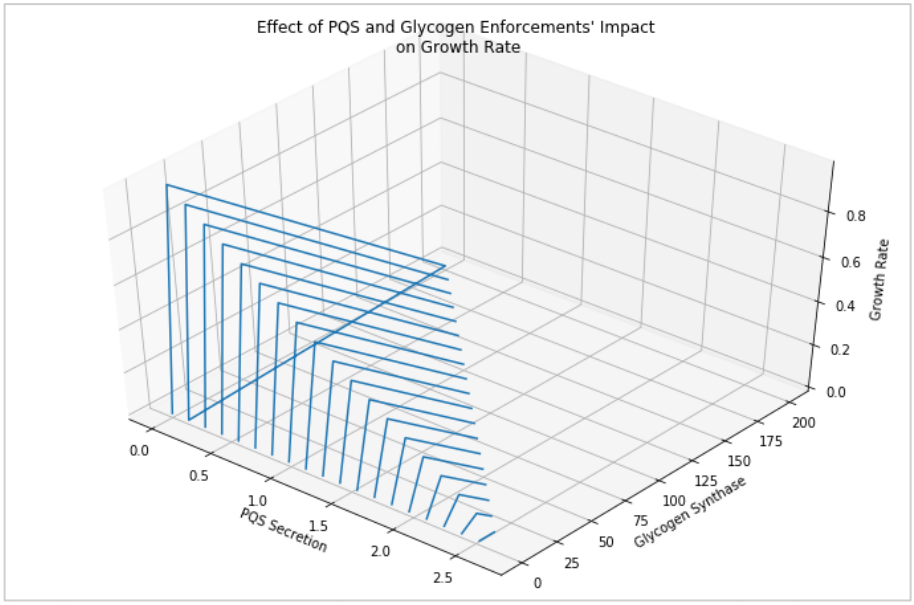

Figure 3.2: Effect of PQS secretion and glycogen synthase on growth rate of *P. aeruginosa.*

3.2. One-Species Temporospatial Modelling Results

3.2.1. Proliferation of *P. aeruginosa* Across the Space

The purpose of this thesis is to establish a multi-scale mathematical modelling of a biofilm under quorum sensing mechanisms using dFBA. Results obtained via the temporospatial biomass growth model of *P. aeruginosa* shown in Figure 3.3.

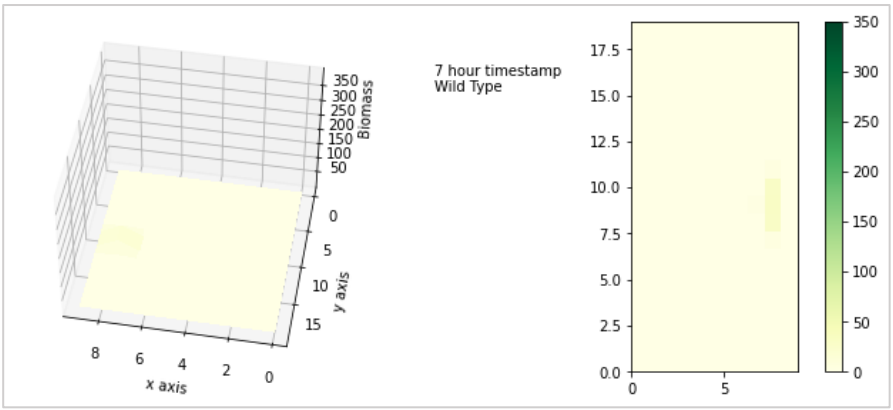

Figure 3.3: *P. aeruginosa* biomass maps : x=10 is the wound surface, snapshots taken at the 7th, 17th and 27th hours respectively.

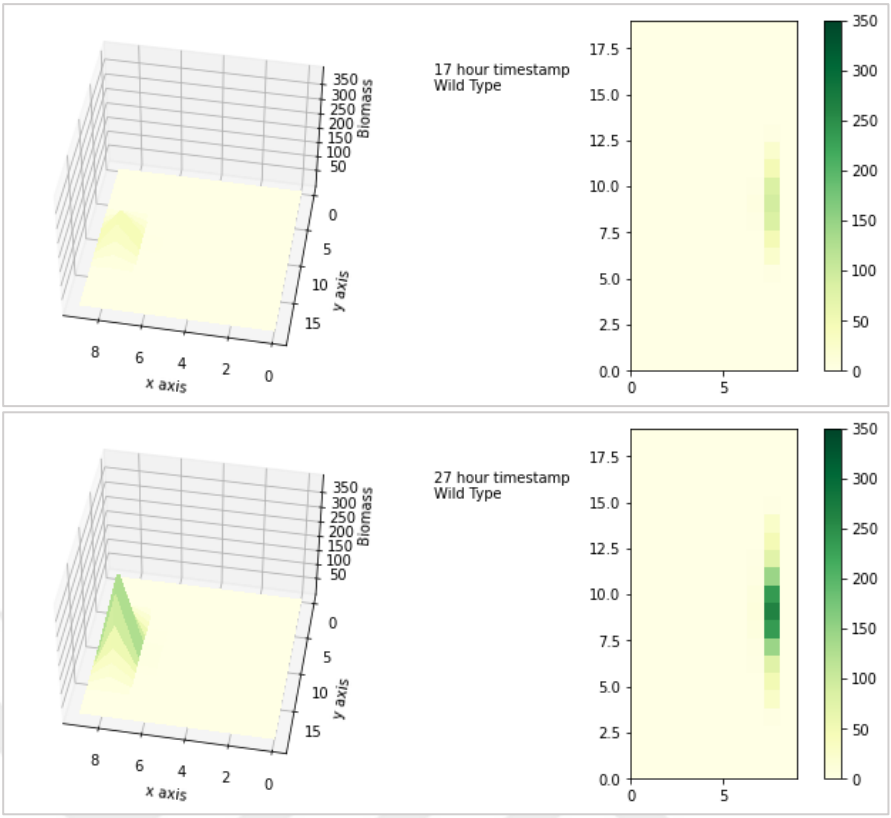

Figure 3.3: Continued.

3.2.1.1. QS Mechanism

Observed growth rate and doubling time is consistent with the literature, which is 2 hours of time for growing two-fold [124]. Comparing the growth before and after QS mechanism being triggered, in a specific lattice location at (8,10), it is observed that the biomass is indeed curbed (Figure 3.3).

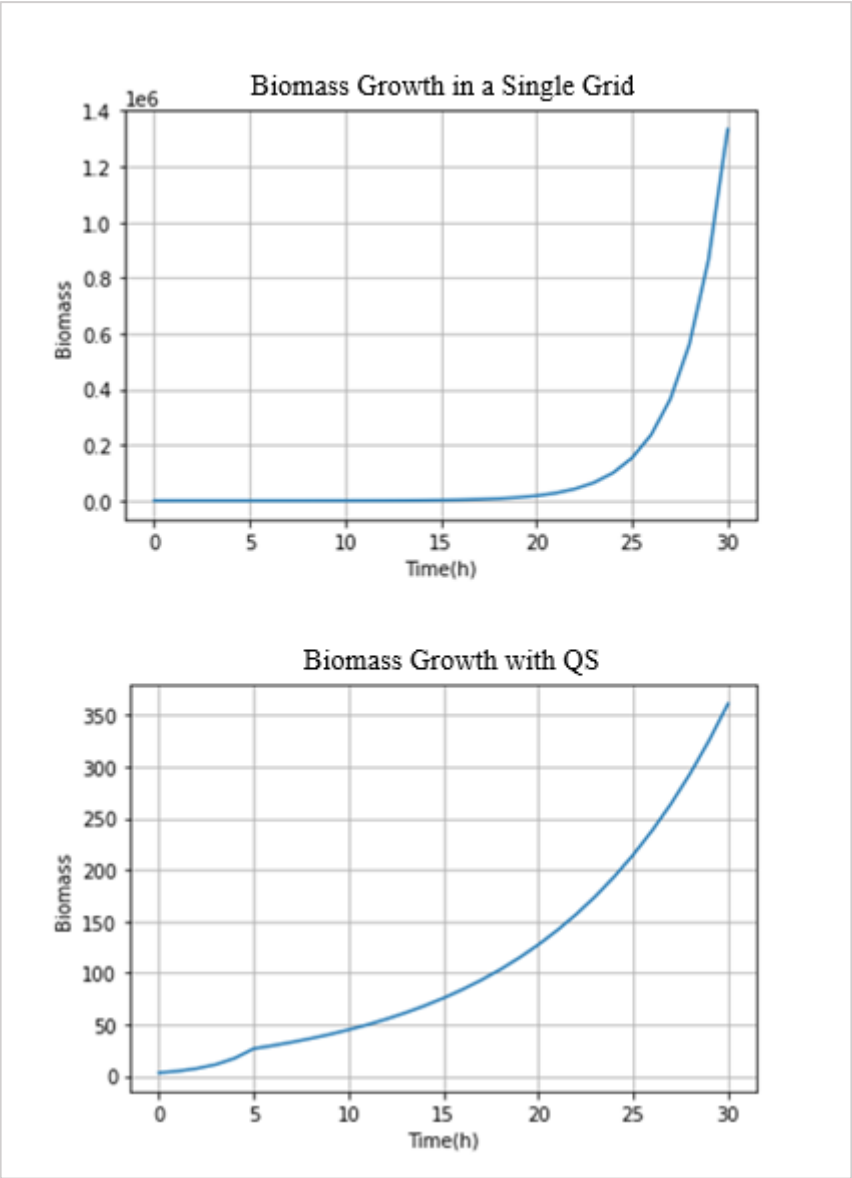

Figure 3.4: A) Biomass growth with no QS restriction B) Biomass growth with QS mechanisms triggered.

The proliferation without an active QS mechanism is seen in Figure 3.5 which reaches the accumulated bacterium mass in Figure 3.3 almost three times faster, which is on par with the literature [125].

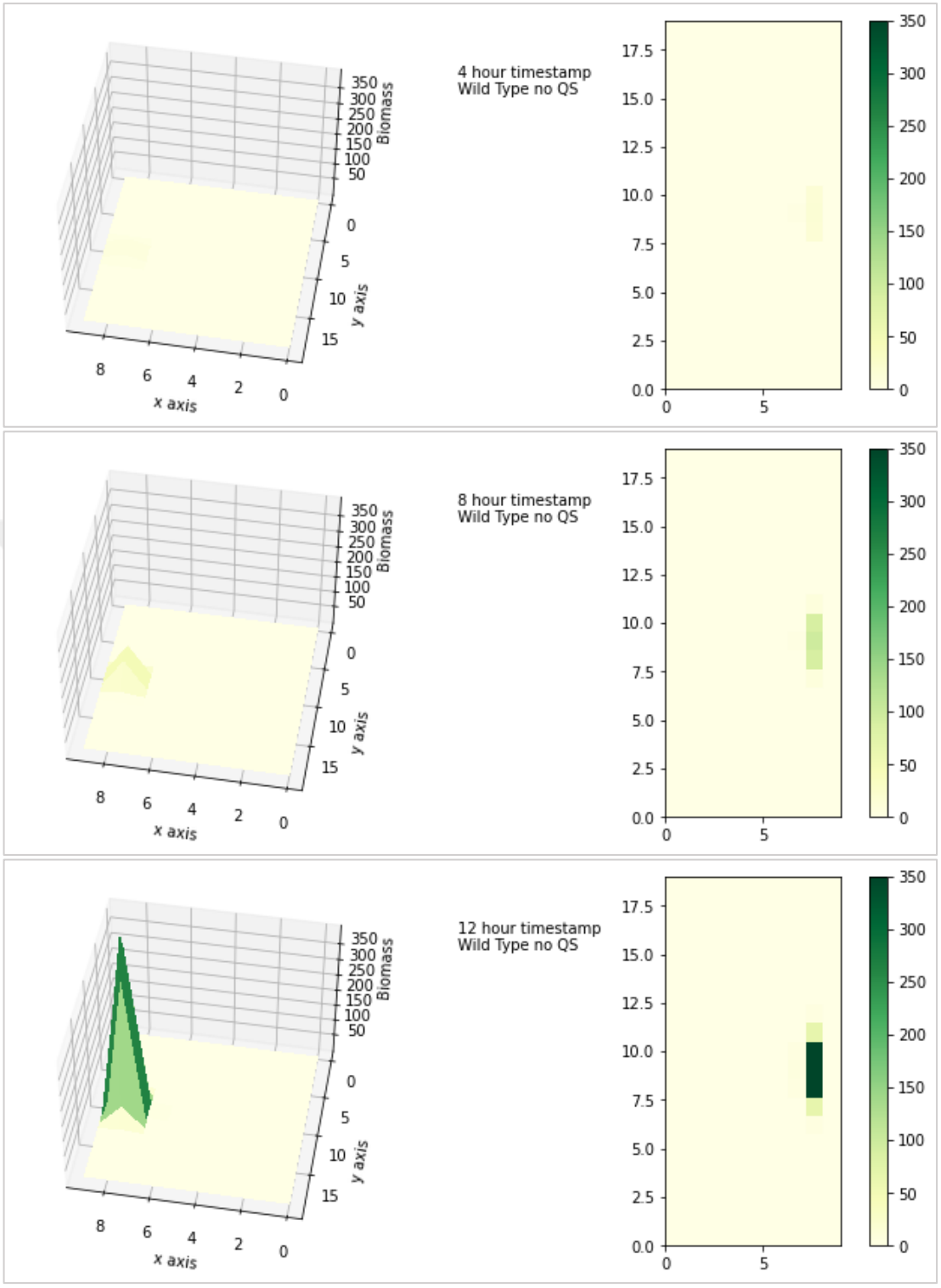

Figure 3.5: *P. aeruginosa* biomass maps : x=10 is the wound surface, snapshots taken at the 4th, 8th and 12th hours respectively under no QS effect.

3.2.1.2. Growth on Chronic Wound

Based on the metabolite levels in blood serum available on "The Human Metabolome Database" for diabetes mellitus patients, the model yields growth profiles which can be seen below in Figure 3.6, respective to the literature, with a growth rate three times faster on chronic wounds when compared to growth observed on an ordinary wound [125].

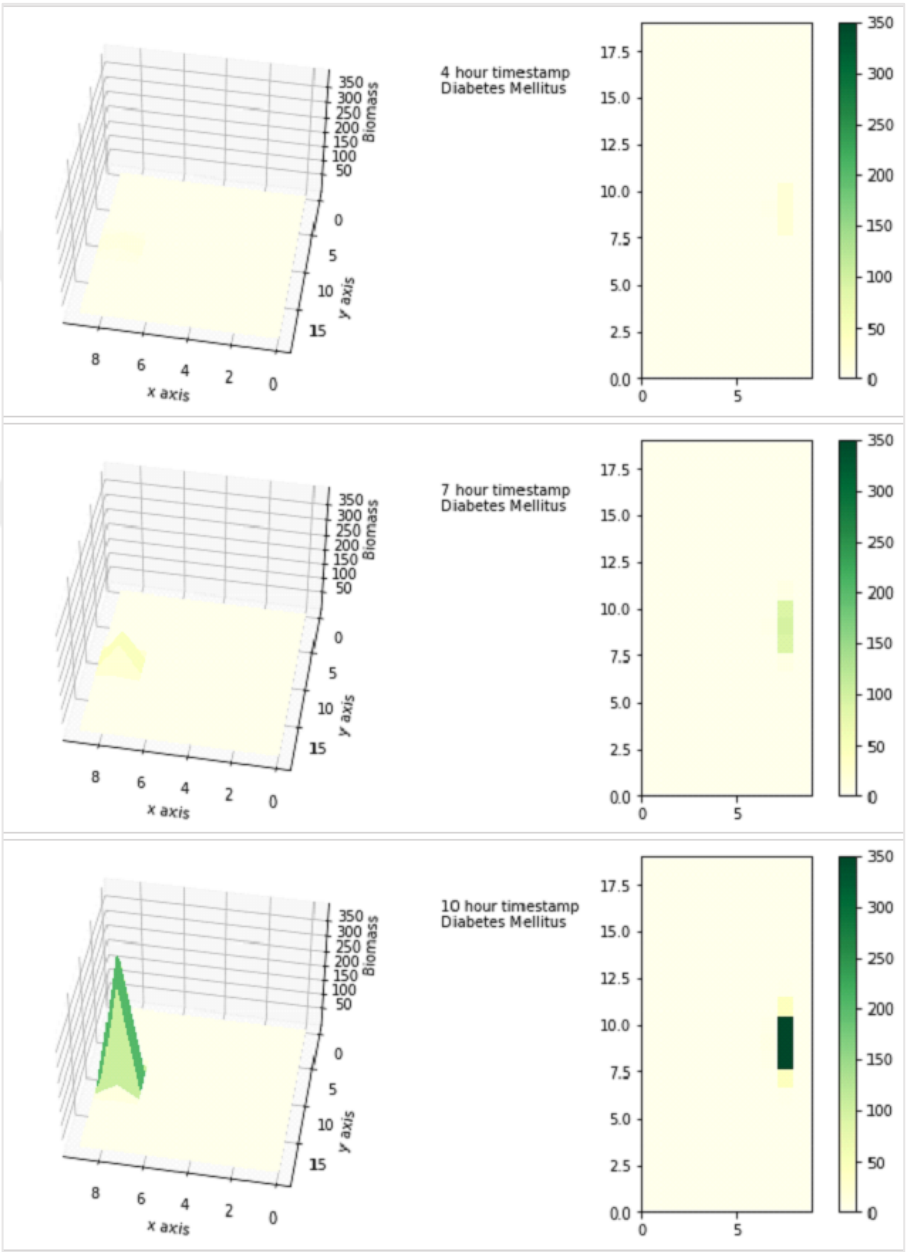

Figure 3.6: *P. aeruginosa* biomass maps : x=10 is the wound surface, snapshots taken at the 4th, 7th and 10th hours respectively on chronic wound.

3.2.1.3. Growth Comparison

In order to compare the growth under three different conditions, with QS mechanisms, without QS mechanisms and chronic wound, growth in a single grid at (8,10) in the central location of the initial point is portrayed (Figure 3.7). The values for three different conditions are subjected to log2 transformation, being 7, 17 and 19 respective to the condition. Transformed total biomass amounts are represented in the image with scaled circle sizes and bacteria amounts, respectively.

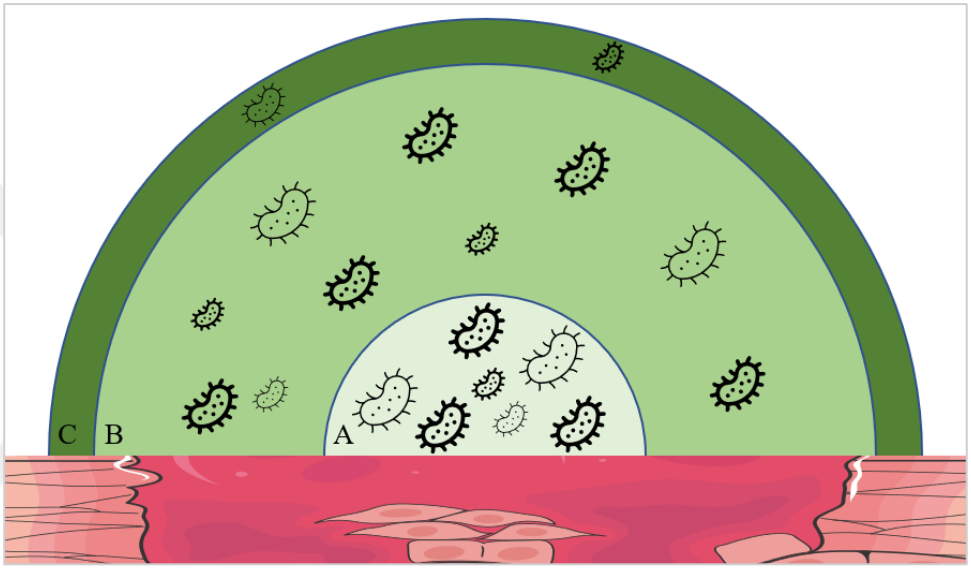

Figure 3.7: A. Biomass Growth subject to QS mechanism, B. Biomass Growth without QS mechanism, C. Biomass Growth on a Chronic Wound.

3.2.1.4. Gene Enrichment Analysis

3.2.1.5. Biofilm Formation and Growth Rate

Performing single gene knockouts to analyse the model and genes given on Table 2.1 which are model genes related to QS mechanisms, only one gene, glgA was found to affect the biomass formation, and the gene, glgA is involved in phenazine biosynthetic process. Later research in the literature revealed that, while it does not affect the adhesion to a surface, its deficiency results in impaired biomass formation [126].

3.2.1.6. QS Related Mechanisms

When comparing reaction fluxes before and after QS mechanisms are triggered in the forementioned lattice, several reactions were observed to have changed drastically. Table 3.1 presents the reactions, together with the genes that encode their enzymes, flux values before and after QS is triggered, and ratio of their fold change to expected fold change (0.25) in response to QS trigger.

Table 3.1: Reactions modulated by QS trigger and their respective regulator genes.

IDs	Regulatory Gene IDs	QS-	QS+	FC
EX_n2_e		0.00000	0.00523	-
EX_nh4_e		-0.12700	0.00000	-
EX_urea_e		-1.37006	-0.36753	0.93193
ACGK		0.26420	0.03968	1.66455
ACOTA	PA5323	-0.26420	-0.03968	1.66455
AGPR	PA0662	-0.26420	-0.03968	1.66455
AKGD	PA1585,PA1586, PA4829	0.06827	0.05315	0.32115
ANO2i	PA1780,PA1781	0.04180	0.00000	-
G5SD	PA4007	0.00000	0.02637	-
GLU5K	PA4565	0.00000	0.02637	-
HCO3E	PA2053	0.96488	0.28831	0.83667
ICDHy	PA2623	-0.14431	0.00000	-
ICL	PA2634	0.14431	0.00000	-
LLEUDr	PA3418	0.00000	-0.01374	-
MALS	PA0482	0.14641	0.00053	69.72015
MDH	PA1252	0.71208	0.14194	1.25417
N2t		0.00000	0.00523	-
NAt7	PA3660,PA3887,PA5021	-0.43615	-0.15687	0.69506
NH4OHD		0.04180	0.00000	-
NH4t	PA3039,PA5287	0.12700	0.00000	-
NIR	PA0514, PA0516, PA0519	0.00000	0.01045	-
NOR	PA0523,PA0524	0.00000	0.00523	-
NOSR	PA3392	0.00000	0.00523	-
ORNTA	PA0895	0.10548	0.00000	-
ORNTAC	PA4402	0.26420	0.03968	1.66455
PC	PA1400	0.00000	0.04709	-
PDH	PA3416,PA3417,PA4829 ,PA5015,PA5016	7.62013	1.86112	1.02360
PPC	PA3687	0.04405	0.00000	-
SUCOAS	PA1588,PA1589	0.00000	-0.03608	-

The genes given above were also held subject to GO analysis and it was found that leucine transport and proline biosynthetic process is activated under QS effects (Figure 3.8).

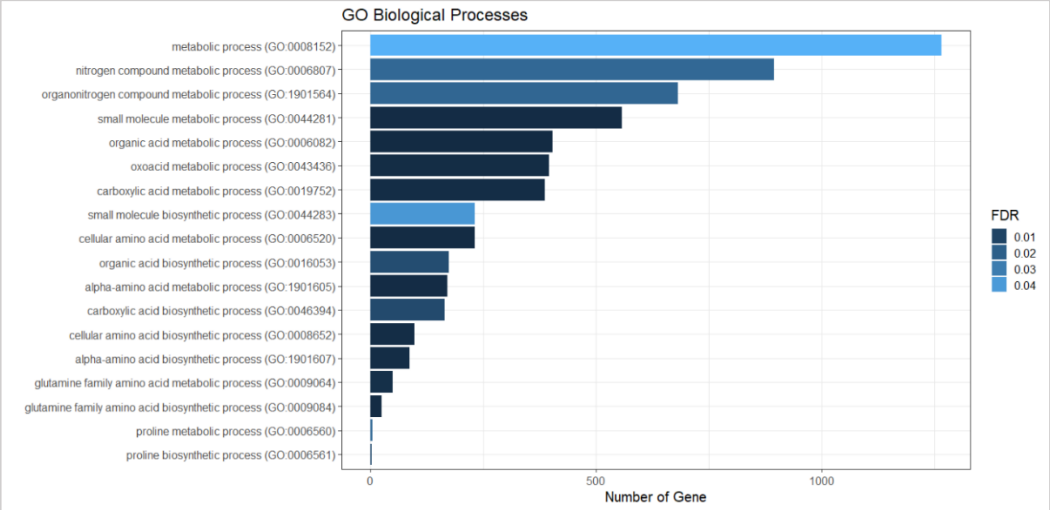

Figure 3.8: Gene Enrichment Analysis for genes listed in Table 3.1.

The result indicates activity leaning toward protein synthesis, consuming available amino acids. Lower metabolite intake of bacteria under QS triggered conditions lead to differential nitrogen regulation and hence, nitrogen cycled via l-glutamate production is also reduced.

3.2.1.7. Metabolite Consumption and Aggregation

Although some of the metabolites available for uptake are included in the model exchange reactions, the model can either fail to fully consume or secrete those metabolites as seen on Table 3.2.

Table 3.2: Metabolites accumulated in the environment and uptake rates of the biomass at (8,10) for a single iteration after QS is triggered.

Metabolites	Remaining Quantity	Secretions	Uptakes
h2o	1705000	12.6185	0
co2	806	9.28832	0
urea	92.8929	0	1.43357
ala_L	13.7826	0.37096	0
ala_D	13.2432	0.64760	0
pi	11.7516	0	0.42868
cys	3.85027	0	0.08366
orn_L	2.90780	0.12950	0
trp_L	1.53832	0	0.02712
ac	1.29890	6.30350	0
lys_L	1.02777	0	0.16374
spmd	0.20353	0	0.00352
tyr_L	0.18607	0	0.06580
ala_B	0.08914	0	0.00003

Table 3.3 presents the list of metabolites that are not consumed by the model in chronic wounds. The list is mostly made of minerals, which are abundant in blood.

Table 3.3: Metabolites not consumed by the model.

Metabolite	Quantity	Metabolite	Quantity
na1	434	myrt	0.77500
fe2	292.980	succ	0.72850
k	130.200	cu2	0.52700
xyl_D	75.7361	fe3	0.51770
lac_L	46.8100	chol	0.44950
ppn	39.8350	zn2	0.41850
hdca	33.0026	hxan	0.34100
mg2	25.8230	prolb	0.31000
so4	15.1900	orot	0.15500

Table 3.3: Continued.

Metabolite	Quantity	Metabolite	Quantity
ocdca	14.4925	4hbz	0.07440
val_L	7.22300	ser_D	0.07130
pro_L	6.14730	acald	0.03100
taur	5.02200	glutar	0.02480
nh4	3.93700	ade	0.01860
cyst	3.37900	ni2	0.01860
glyb	2.54200	4abut	0.01550
man	1.98400	mn2	0.00620
ascb	1.88480	ptrc	0.00310
crn	1.33300	thm	0.00310
no2	0.99200		

3.2.2. Proliferation of S. aureus Across the Space

Results obtained via the temporospatial biomass growth model of *S. aureus* are represented in Figure 3.9. In the model, QS and reduction of diffusion due to biofilm formation is triggered via mimicking the mechanism of *P. aeruginosa*. Separate models for chronic wounds yielded identical results as wild type. Further investigation revealed that phosphate availability was the limiting factor, therefore higher glucose levels had no further effect on the growth. The model's dependency on phosphate levels is a result of high demand for phosphate in the biomass equation.

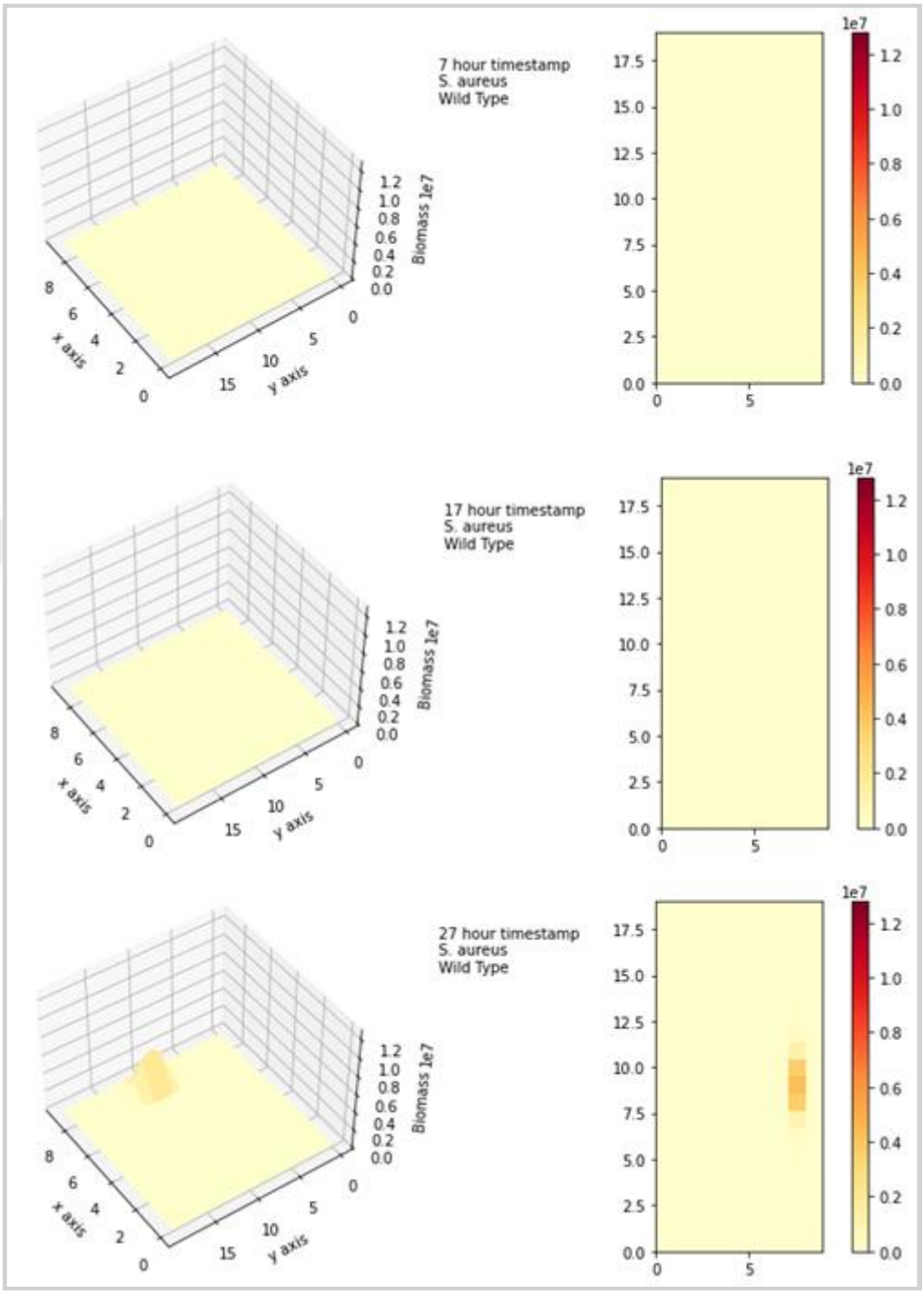

Figure 3.9: *S. aureus* biomass maps : x=10 is the wound surface, snapshots taken at the 7th, 17th and 27th hours respectively on a chronic wound.

3.3. Two-Species Temporospatial Modelling Results

3.3.1. Proliferation Across the Space

Maps of growth across the lattice for the combined model of *P. aeruginosa* and *S. aureus* are presented in Figure 3.10. Both species are seeded in the same grids initially and allowed to grow based on their respective metabolic models. The model of *S. aureus* yields higher biomass rate compared to *P. aeruginosa* under normal glucose conditions, which is visible at the peak levels of both species.

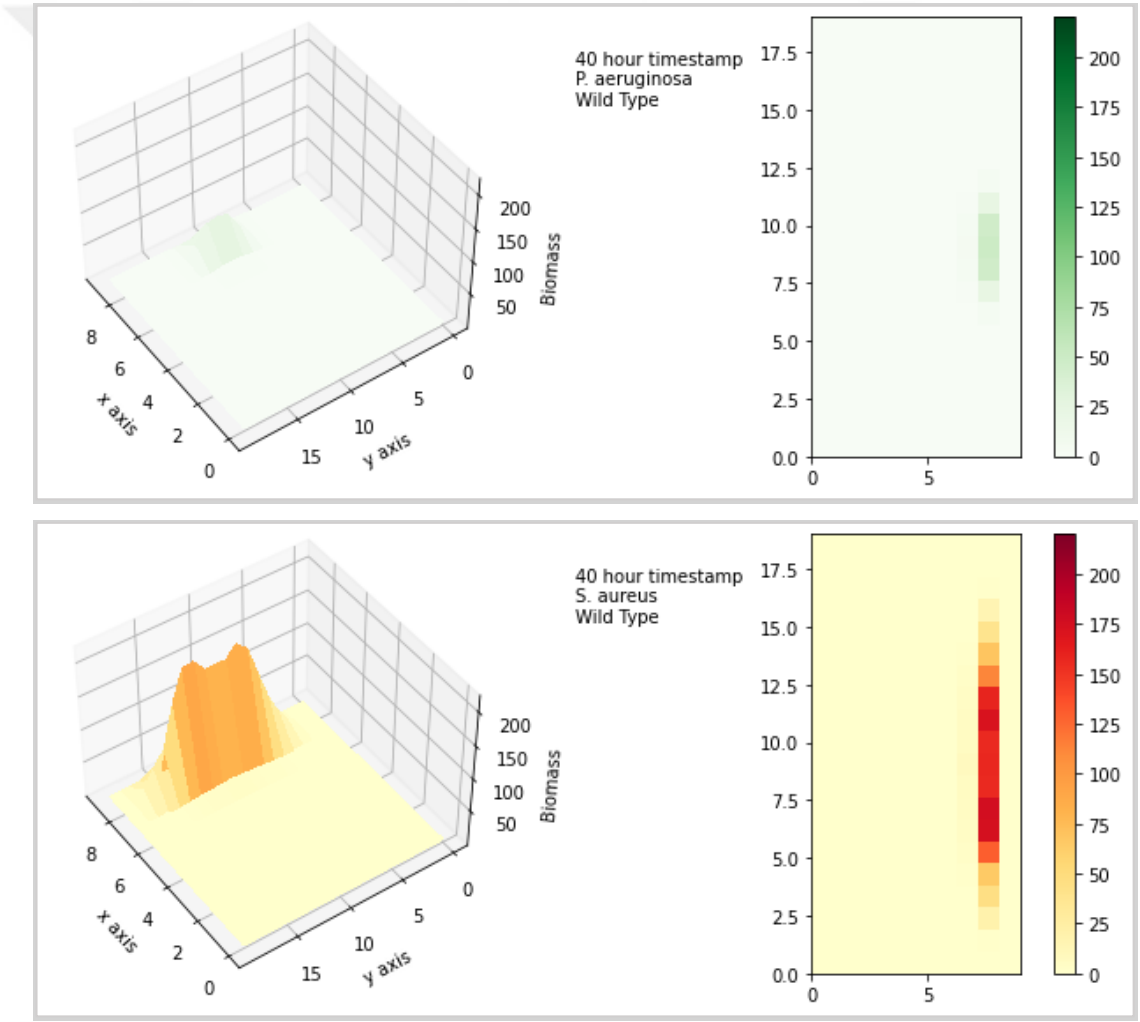

Figure 3.10: Combined biomass maps : x=10 is the wound surface, snapshots taken at the 40th, 80th and 120th hours respectively. (Continuous to the next page).

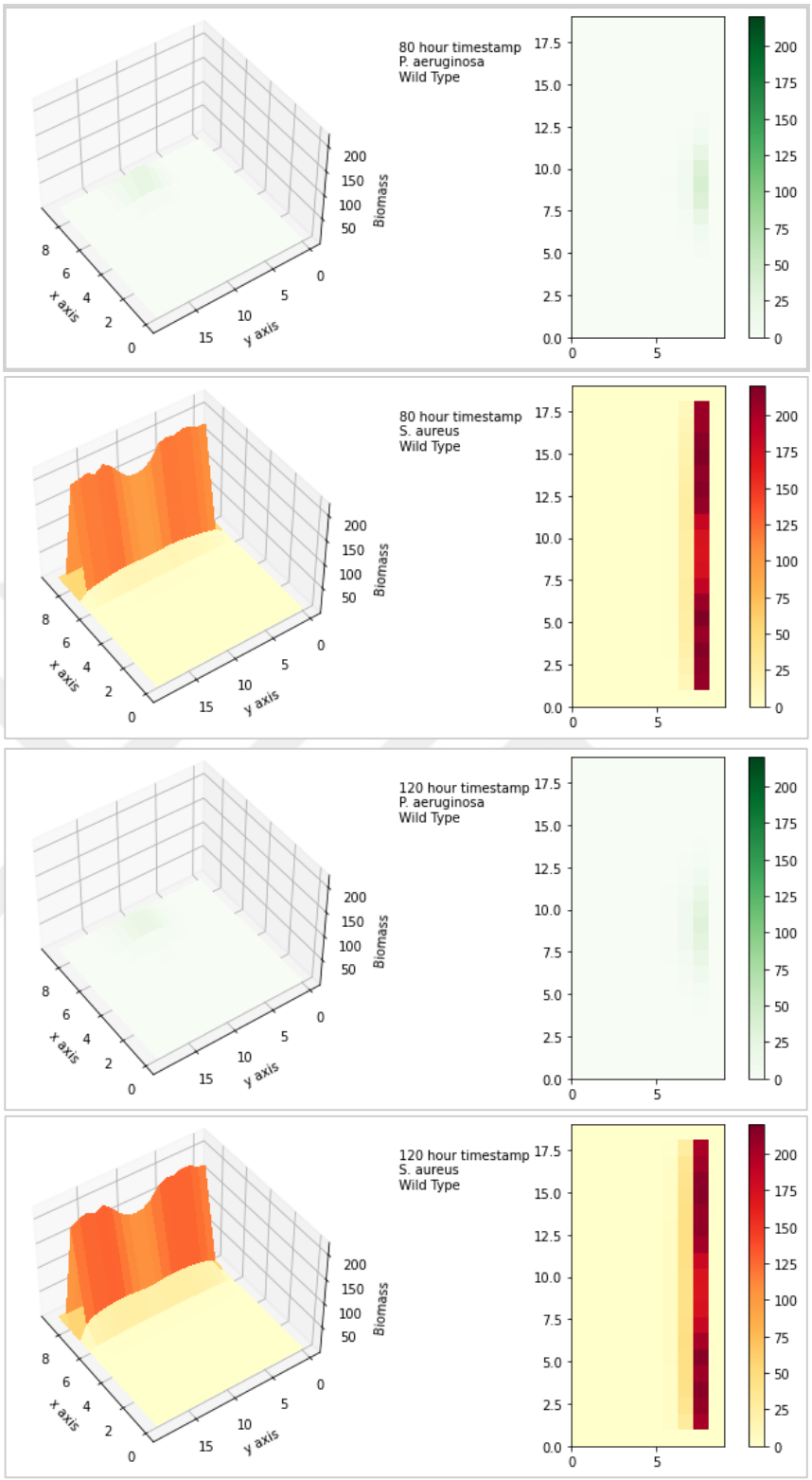

Figure 3.10: Continued.

3.3.2. Growth on Chronic Wound

On chronic wounds however, the proliferation map of both species yields results switched over in terms of growth. *P. aeruginosa* being better at utilizing glucose in its GMN, while *S. aureus* is suffering from phosphate starvation due to the biomass equation in its GMN, is the result driven from further inspection of both models.

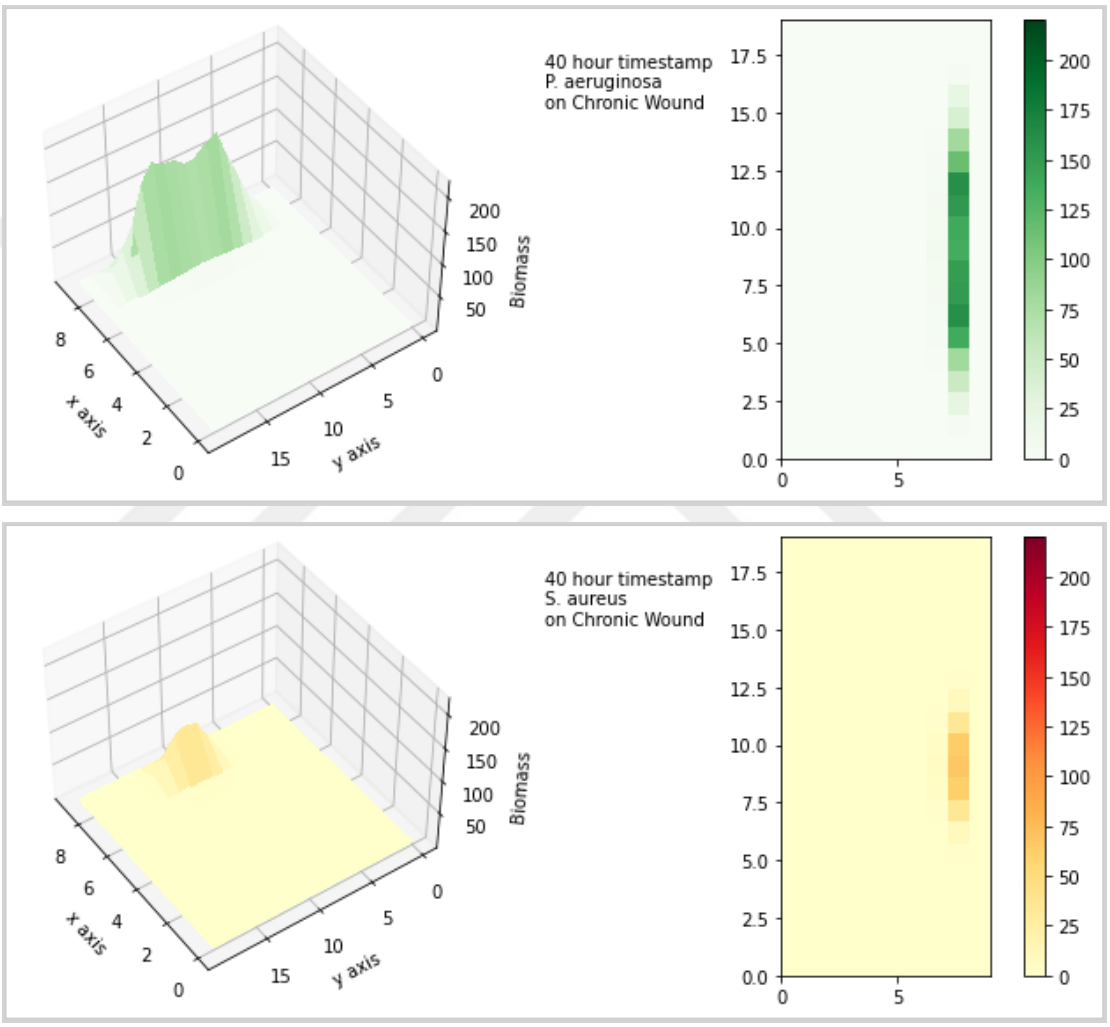

Figure 3.11: Combined biomass maps : x=10 is the wound surface, snapshots taken at the 40th, 80th and 120th hours respectively on chronic wound (Continues on the next page).

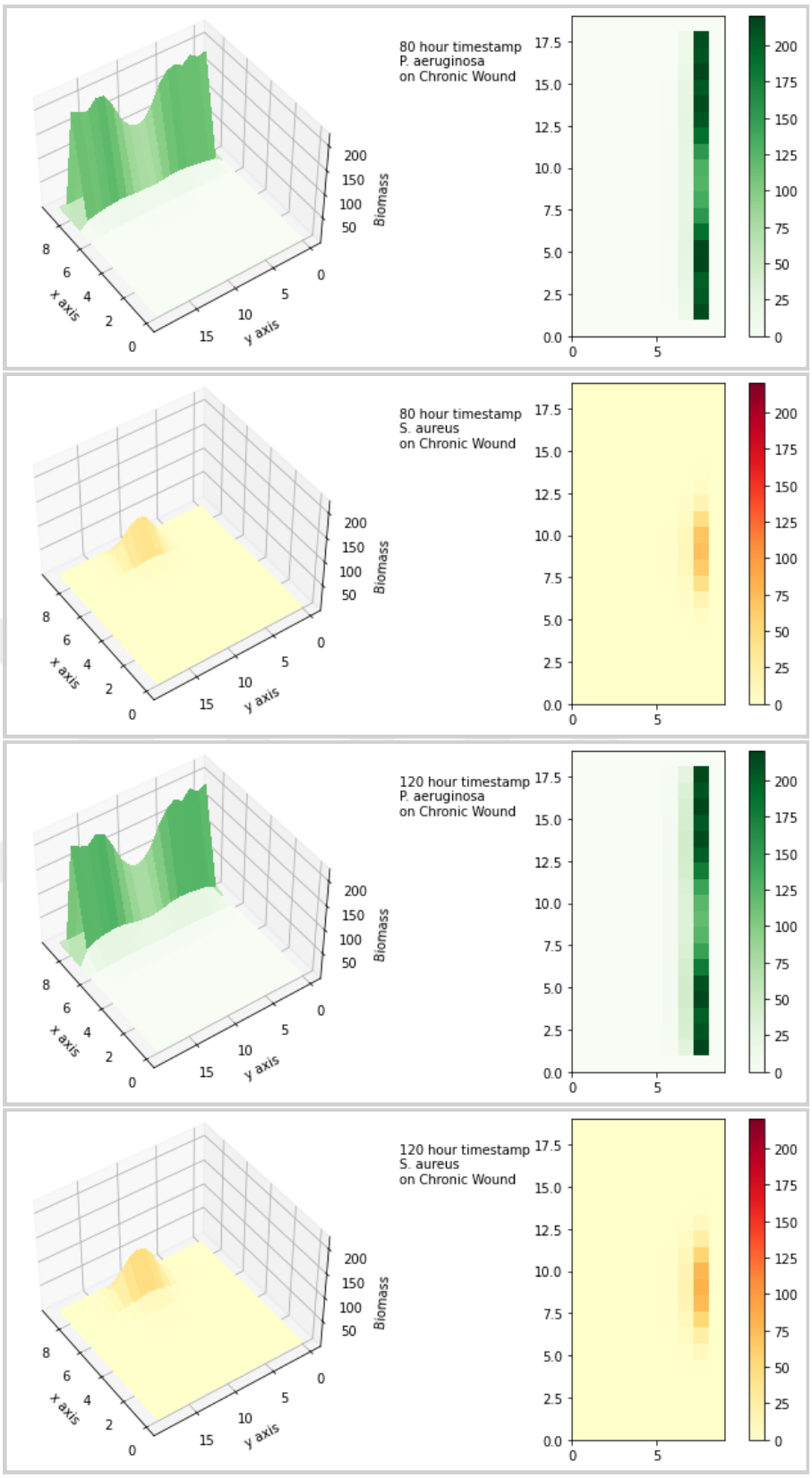

Figure 3.11: Continued.

3.3.2.1. Initial Biomass Location Trials on Chronic Wound

Changing the initial points of *P. aeruginosa* so that it would be surrounding *S. aureus*, instead of being seeded in the same grid, resulted in both species vaguely establishing their territories before stabilizing in a mixed grid. As seen in Figure 3.11, compared to the mixed location maps, *S. aureus* is better at showing growth in its central initial location.

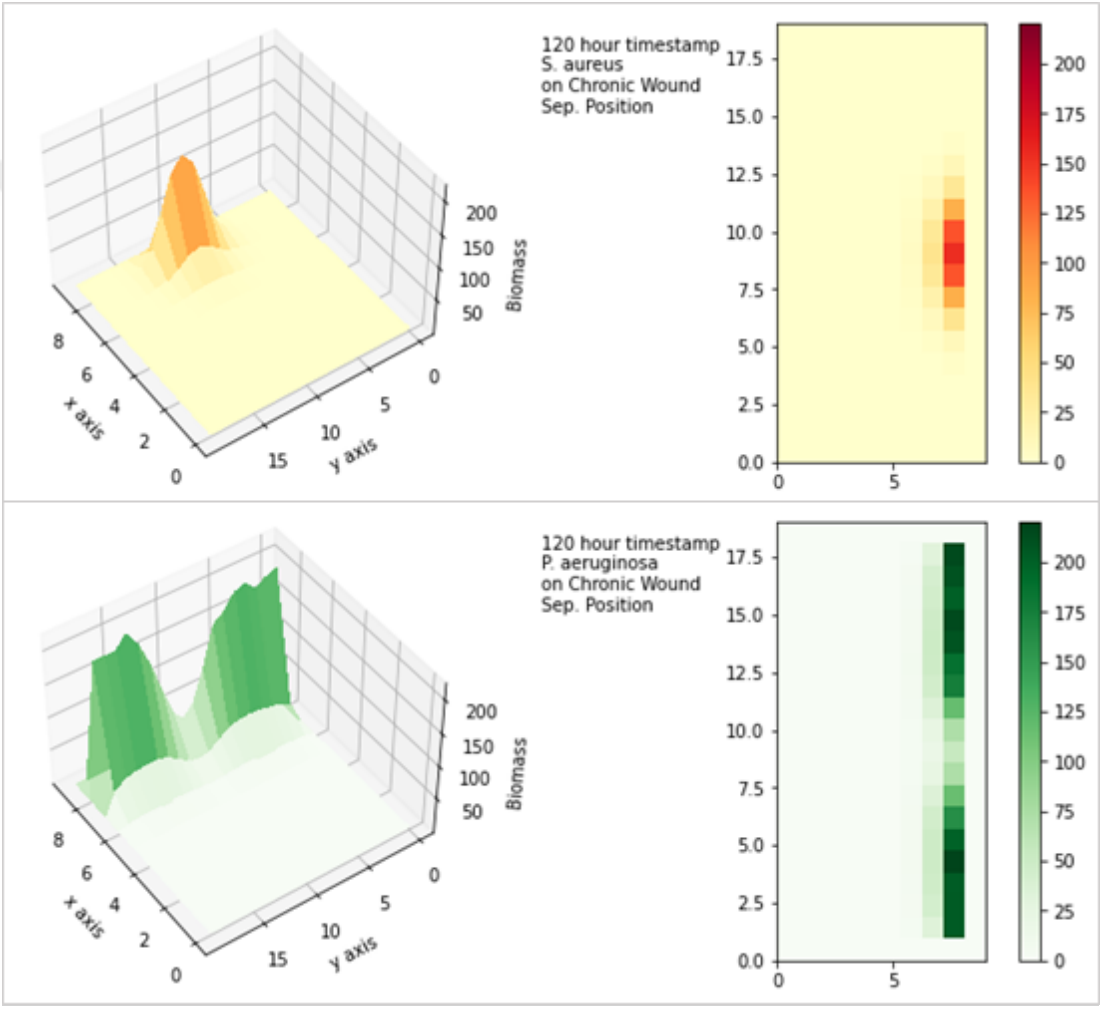

Figure 3.12: Combined biomass maps : x=10 is the wound surface, snapshots taken at 120th hour on chronic wound with separate initial locations.

3.3.2.2. Pyocyanin Trials on Chronic Wound

In order to test the effect of different pyocyanin levels to see the impact of increased antibiotic secretion of *P. aeruginosa* and its effect on *S. aureus*, two different trials are carried out, reducing the impact by half and doubling it. The maps represented in Figure 3.11 are showing that the model works as intended regarding pyocyanin, reducing growth rate of S. aureus, being an antibiotic effective against it.

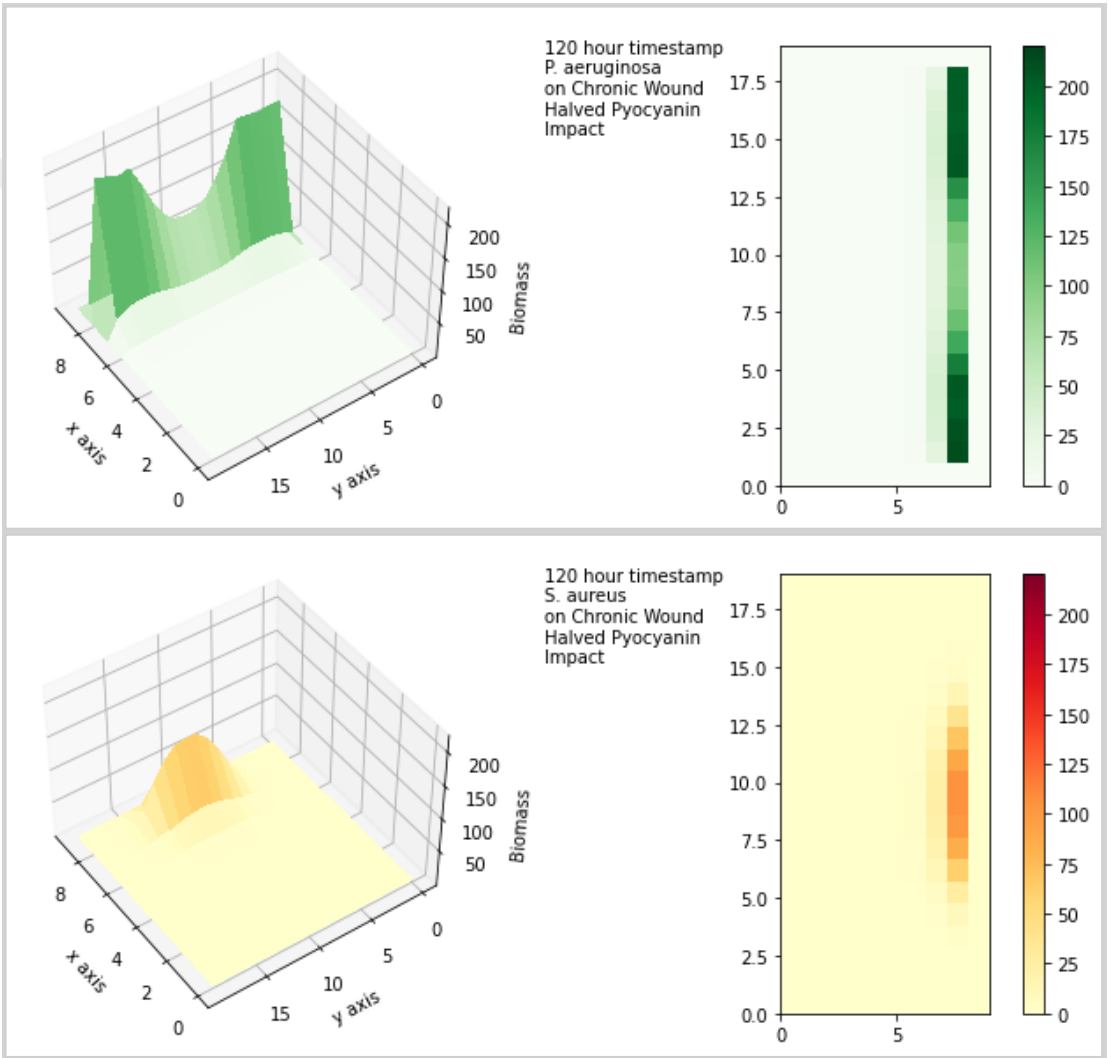

Figure 3.13: Combined biomass maps : x=10 is the wound surface, snapshots taken at 120th hour on chronic wound with halved pyocyanin impact.

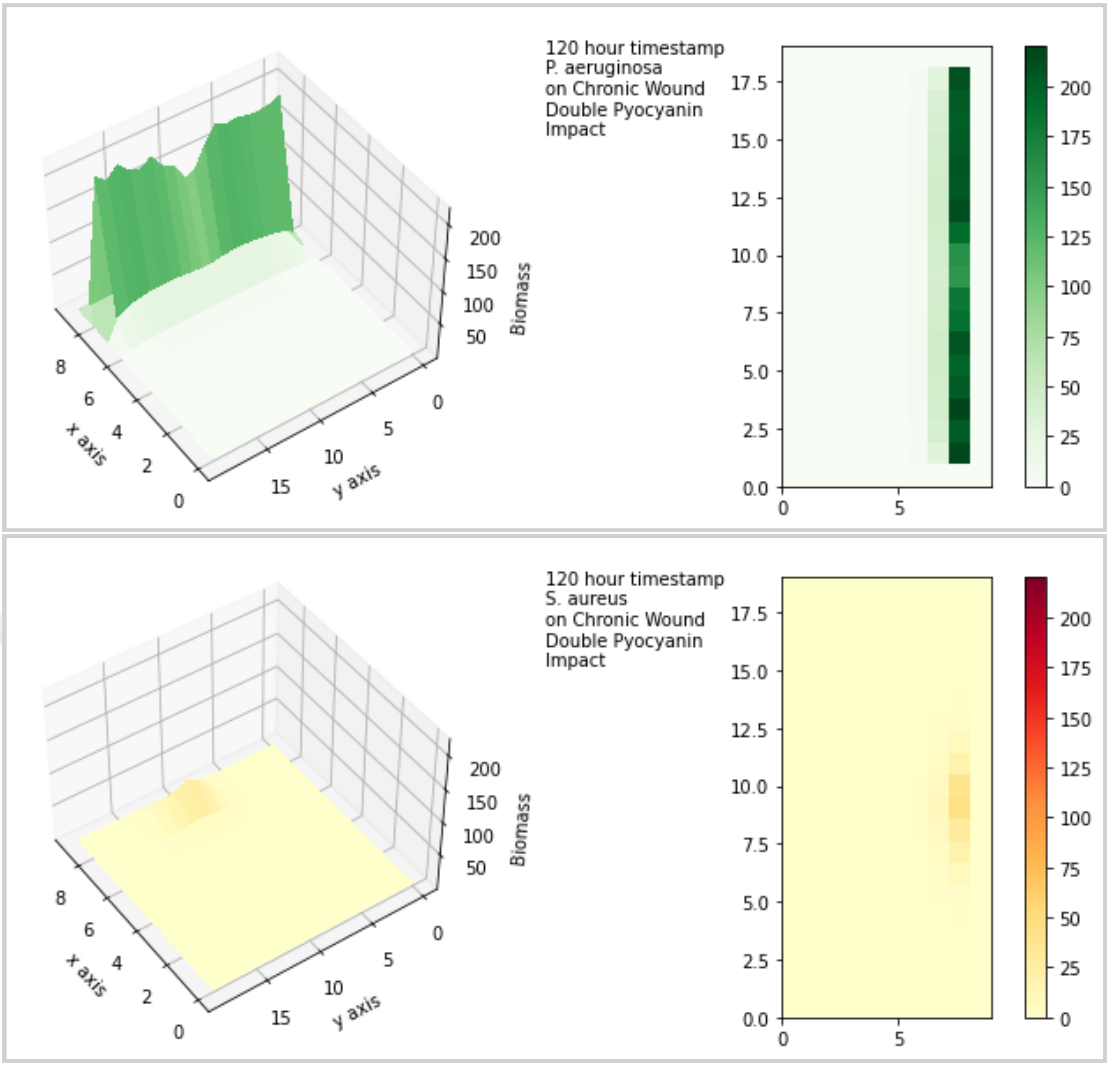

Figure 3.14: Combined biomass maps : x=10 is the wound surface, snapshots taken at 120th hour on chronic wound with doubled pyocyanin impact.

4. DISCUSSION

In this thesis, it is aimed to model and observe *P. aeruginosa* growth under quorum sensing mechanism to better understand the bacterial infestation, further enhanced by addition of *S. aureus* model and their combined two-species model. The multiscale model could make accurate predictions, reflecting both hindered and unhindered growth and many changes in metabolism on par with the literature.

4.1. Chronic Wounds

For metabolite concentrations taken for the chronic wound case, only glucose is altered to differentiate between regular growth. This is due to two factors, first is lack of detailed experimental data and the latter is that a study supporting that amino acid levels do not change in type II diabetes with respect to healthy individuals [127].

When the bacteria on chronic wounds are isolated, *Staphylococcus aureus* is most commonly in partnership with *Pseudomonas aeruginosa* [128]. As these bacteria have a mutual relationship, the former being an anaerobic species while the latter favouring oxygen-rich environment, it is vital to establish a model that facilitates this mutuality, however due to limitations of available GMNs of species, phenomena such as tobramycin resistance gained by *P. aeruginosa* could not be simulated.

Single-species models do not have a biomass upper limit per lattice, and it is observed that *S. aureus* grows much more rapidly compared to *P. aeruginosa*. Their combined growth model however, being reversed in growth rates according to the results, when chronic wound conditions were introduced could better be explained by *P. aeruginosa* model being better at utilizing glucose, while *S. aureus* being more opportunistic in harsher conditions.

In the making of this temporospatial model, it is observed that the initial points of biomass assigned to species plays a big role in the result. In a real-life scenario, a space could not be filled with two masses at the same time but programming the lattice as a real-life space is a much harder problem, so it is assumed that the spaces are automatically filled with available biomass and an upper limit is introduced for each grid according to a general biomass amount that could hold a specific amount of space and then the growth is modelled accordingly.

4.2. Quorum Sensing

The model uses a certain biomass quantity to be the threshold for triggering QS mechanisms, reducing the diffusion rates of metabolites in the environment as if the bacteria in a given lattice is already surrounded by biofilm. It should be kept in mind that biofilm formation is not an instant occurrence, and its formation as well as phases it goes through had to be ignored in this model, as there is no secretion and uptake of autoinducers included within the reactions. Hence, changing PQS bounds in the GMN could not be fully exploited.

On metabolites, a sharp drop in ACGK (l-arginine) is observed, given on Table 3.1, which could be due to reduced l-glutamate production, l-arginine being a precursor of l-glutamate. As l-glutamate contain nitrogen which could be transferred for other biosynthesis pathways, a drop in biomass growth yields is an expected result of reduction in l-glu production [129]. Reduction in ACOTA (Acetylornithine transaminase) [130], downregulation of sucB gene which encodes AKGD (2-oxoglutarate dehydrogenase) as it is part of the TCA cycle [131] are also expected results for *P. aeruginosa* biofilms. It should also be mentioned that l-glutamate is synthesized directly from 2- oxoglutarate, an intermediate metabolite in TCA cycle.

Analysis on gene level could not be done for *S. aureus* because the model did not include genes assigned to the reactions. *P. aeruginosa* being studied more commonly in single species biofilms but unavailability of information on *S. aureus* in that regard also resulted in the study being tailored for available information, *ie.*, same rates and numbers applied for both species.

4.3. Biomass Proliferation and Metabolite Diffusion

The proliferation and metabolite diffusion processes are done by discretization partial differential equations. This resulted in the biomass and metabolites to be able to move only one grid at a given iteration, which could be either horizontal or vertical. As a result, biomass breaking away from biofilm or surges of bacteria could not be represented.

Although there are studies about biofilms and their metabolic permeability, taking easiness and technical availability into consideration, mostly water and glucose

fluxes are studied. Glucose flux rates are taken as a major reference point in this study. Hence, finding appropriate flux rates for each available metabolite requires exhaustive wet lab experiments to improve the liability of this model.

Another phenomena that is not represented in the model is the bacterial movement that is not caused by its twitching movement. Any other mechanical interruption, such as scratching, rubbing etc. or the movement through the serum had to be ignored, as diffusion rates for such phenomena are not available, and any assumption made would solely affect the outcome directly. The diffusion rate of *P. aeruginosa* and *S. aureus* themselves are not enough to achieve a portrayal of a petri dish result, as the mass accumulates at its initial point, instead of following a tendency to migrate or being washed away by movement of fluids.

5. CONCLUSION

Accurate modelling of biofilms is needed to study their mechanisms in order to obtain possible ways to promote or suppress them according to the biological problem of interest. To derive such insight, a growth model of *P. aeruginosa* and *S. aureus* was computationally modelled in this thesis. Bacterial regulations driven by Quorum Sensing effects, which is how bacteria "count" the population and phase into a defensive mode. Genome-Scale Metabolic Network analysis was conducted in order to observe how a small infection grew into a larger mass of bacterium, using FBA, temporospatial modelling and quorum sensing scales. Results matching ontological findings in literature were obtained. Both initial infection and inter-species relations are studied and represented for several cases in this study, which might shed light on mechanisms of the clinical observations on both bacteria. Effects of different antibiotics which focuses on killing bacteria themselves or hindering their biomass formation or its complete abolishment could further be introduced to the system to analyse and learn the behaviour of *P. aeruginosa* and *S. aureus* to help clinicians fight the organisms more effectively.

REFERENCES

[1] Venkova T., Yeo C. C., Espinosa M., (2018), "Editorial: The Good, The Bad, and The Ugly: Multiple Roles of Bacteria in Human Life", Front Microbiol, 9.

[2] Lawrence J. R., Korber D. R., Hoyle B. D., Costerton J. W., Caldwell D. E., (1991), "Optical sectioning of microbial biofilms", J Bacteriol, 173(20), 6558–6567.

[3] Eberl H. J., Parker D. F., Vanloosdrecht M. C. M., (2001), "A new deterministic spatio-temporal continuum model for biofilm development", J Theor Med, 3(3), 161–175.

[4] Singh S., Singh S. K., Chowdhury I., Singh R., (2017), "Understanding the Mechanism of Bacterial Biofilms Resistance to Antimicrobial Agents", Open Microbiol J, 11(1), 53–62.

[5] Costerton J. W., (1999), "Introduction to biofilm". In: International Journal of Antimicrobial Agents. Int J Antimicrob Agents, pp 217–221.

[6] Luo J., Lv P., Zhang J., Fane A. G., McDougald D., Rice S. A., (2017), "Succession of biofilm communities responsible for biofouling of membrane bioreactors (MBRs)", PLoS One, 12(7), e0179855.

[7] Boomer S. M., Noll K. L., Geesey G. G., Dutton B. E., (2009), "Formation of multilayered photosynthetic biofilms in an alkaline thermal spring in Yellowstone national Park, Wyoming", Appl Environ Microbiol, 75(8), 2464–2475.

[8] Koerdt A., Gödeke J., Berger J., Thormann K. M., Albers S.-V., (2010), "Crenarchaeal Biofilm Formation under Extreme Conditions", PLoS One, 5(11), e14104.

[9] Moslemy P., Neufeld R. J., Guiot S. R., (2002), "Biodegradation of gasoline by gellan gum-encapsulated bacterial cells", Biotechnol Bioeng, 80(2), 175–184.

[10] NIH Guide: Research on Microbial Biofilms, (2002), https://grants.nih.gov/grants/guide/pa-files/PA-03-047.html, (Accessed 24 Nov 2021).

[11] Rumbaugh K. P., Sauer K., (2020), "Biofilm dispersion". Nat. Rev. Microbiol. 18:571–586.

[12] James G. A., Swogger E., Wolcott R., Pulcini E. deLancey, Secor P., Sestrich J., Costerton J. W., Stewart P. S., (2008), "Biofilms in chronic wounds", Wound Repair Regen, 16(1), 37–44.

[13] Stewart P. S., Costerton J. W., (2001), "Antibiotic resistance of bacteria in biofilms". Lancet 358:135–138.

[14] Parsek M. R., Singh P. K., (2003), "Bacterial Biofilms: An Emerging Link to Disease Pathogenesis". Annu. Rev. Microbiol. 57:677–701.

[15] Fux C. A., Costerton J. W., Stewart P. S., Stoodley P., (2005), "Survival strategies of infectious biofilms". Trends Microbiol. 13:34–40.

[16] Bishop P. L., Rittmann B. B., (1995), "Modelling heterogeneity in biofilms: Report of the discussion session", Water Sci Technol, 32(8), 263–265.

[17] Burmølle M., Ren D., Bjarnsholt T., Sørensen S. J., (2014), "Interactions in multispecies biofilms: Do they actually matter?". Trends Microbiol. 22:84–91.

[18] Elias S., Banin E., (2012), "Multi-species biofilms: living with friendly neighbors", FEMS Microbiol Rev, 36(5), 990–1004.

[19] Kolenbrander P. E., (2011), "Multispecies communities: Interspecies interactions influence growth on saliva as sole nutritional source". In: International Journal of Oral Science. Nature Publishing Group, pp 49–54.

[20] Kreth J., Merritt J., Qi F., (2009), "Bacterial and host interactions of oral streptococci.", DNA Cell Biol, 28(8), 397–403.

[21] Sbordone L., Bortolaia C., (2003), "Oral microbial biofilms and plaque-related diseases: microbial communities and their role in the shift from oral health to disease", Clin Oral Investig, 7(4), 181–188.

[22] Elias S., Banin E., (2012), "Multi-species biofilms: Living with friendly neighbors". FEMS Microbiol. Rev. 36:990–1004.

[23] Baille G. S., Berit A., Douglas L. J., (2002), "Mixed species biofilms of Candida albicans and Staphylococcus epidermidis", J Med Microbiol, 51(4), 344–349.

[24] Beaudoin T., Yau Y. C. W., Stapleton P. J., Gong Y., Wang P. W., Guttman D. S., Waters V., (2017), "Staphylococcus aureus interaction with Pseudomonas aeruginosa biofilm enhances tobramycin resistance", npj Biofilms Microbiomes, 3(1), 25.

[25] Kara D., Luppens S. B. I., Van Marle J., Azok R., Ten Cate J. M., (2007), "Microstructural differences between single-species and dual-species biofilms of Streptococcus mutans and Veillonella parvula, before and after exposure to chlorhexidine", FEMS Microbiol Lett, 271(1), 90–97.

[26] Sakai-Kawada F. E., Ip C. G., Hagiwara K. A., Awaya J. D., (2019), "Biosynthesis and Bioactivity of Prodiginine Analogs in Marine Bacteria, Pseudoalteromonas: A Mini Review", Front Microbiol, 10(JULY), 1715.

[27] Peters L., König G. M., Wright A. D., Pukall R., Stackebrandt E., Eberl L., Riedel K., (2003), "Secondary metabolites of Flustra foliacea and their influence on bacteria.", Appl Environ Microbiol, 69(6), 3469–75.

[28] Elias S., Banin E., (2012), "Multi-species biofilms: living with friendly neighbors", FEMS Microbiol Rev, 36(5), 990–1004.

[29] Tolker-Nielsen T., Molin S., (2000), "Spatial organization of microbial biofilm communities", Microb Ecol, 40(2), 75–84.

[30] Liu W., Røder H. L., Madsen J. S., Bjarnsholt T., Sørensen S. J., Burmølle M., (2016), "Interspecific Bacterial Interactions are Reflected in Multispecies Biofilm Spatial Organization", Front Microbiol, 7(AUG), 1366.

[31] Egland P. G., Palmer R. J., Kolenbrander P. E., (2004), "Interspecies communication in Streptococcus gordonii-Veillonella atypica biofilms: Signaling in flow conditions requires juxtaposition", Proc Natl Acad Sci U S A, 101(48), 16917–16922.

[32] Miller M. B., Bassler B. L., (2001), "Quorum Sensing in Bacteria", Annu Rev Microbiol, 55, 165–99.

[33] de Kievit T. R., Iglewski B. H., Kievit T. R. De, Teresa R., (2000), "Bacterial Quorum Sensing in Pathogenic Relationships", Infect Immun, 68(9), 4839–4849.

[34] Goo E., An J. H., Kang Y., Hwang I., (2015), "Control of bacterial metabolism by quorum sensing". Trends Microbiol. 23:567–576.

[35] González J. E., Keshavan N. D., (2006), "Messing with bacterial quorum sensing.", Microbiol Mol Biol Rev, 70(4), 859–75.

[36] Aurich M. K., Thiele I., (2016), "Computational Modeling of Human Metabolism and Its Application to Systems Biomedicine", Methods Mol Biol, 1386, 253–281.

[37] Lupp C., Ruby E. G., (2005), "Vibrio fischeri uses two quorum-sensing systems for the regulation of early and late colonization factors", J Bacteriol, 187(11), 3620–3629.

[38] Stevens A. M., Greenberg E. P., (1997), "Quorum sensing in Vibrio fischeri: essential elements for activation of the luminescence genes.", J Bacteriol, 179(2), 557–62.

[39] De Kievit T. R., Iglewski B. H., (2000), "Bacterial quorum sensing in pathogenic relationships". Infect. Immun. 68:4839–4849.

[40] Eberhard A., Burlingame A. L., Eberhard C., Kenyon G. L., Nealson K. H., Oppenheimer N. J., (1981), "Structural identification of autoinducer of Photobacterium fischeri luciferase", Biochemistry, 20(9), 2444–2449.

[41] Engebrecht J., Silverman M., (1987), "Nucleotide sequence of the regulatory locus controlling expression of bacterial genes for bioluminescence.", Nucleic Acids Res, 15(24), 10455–67.

[42] Bassler B. L., Wright M., Showalter R. E., Silverman M. R., (1993), "Intercellular signalling in Vibrio harveyi: sequence and function of genes regulating expression of luminescence.", Mol Microbiol, 9(4), 773–86.

[43] Bassler B. L., Wright M., Silverman M. R., (1994), "Multiple signalling systems controlling expression of luminescence in *Vibrio harveyi*: sequence and function of genes encoding a second sensory pathway", Mol Microbiol, 13(2), 273–286.

[44] Cao J. G., Meighen E. A., (1989), "Purification and structural identification of an autoinducer for the luminescence system of Vibrio harveyi.", J Biol Chem, 264(36), 21670–6.

[45] Showalter R. E., Martin M. O., Silverman M. R., (1990), "Cloning and nucleotide sequence of luxR, a regulatory gene controlling bioluminescence in Vibrio harveyi.", J Bacteriol, 172(6), 2946–54.

[46] Chapon-Hervé V., Akrim M., Latifi A., Williams P., Lazdunski A., Bally M., (1997), "Regulation of the xcp secretion pathway by multiple quorum-sensing modulons in Pseudomonas aeruginosa.", Mol Microbiol, 24(6), 1169–78.

[47] Gambello M. J., Kaye S., Iglewski B. H., (1993), "LasR of Pseudomonas aeruginosa is a transcriptional activator of the alkaline protease gene (apr) and an enhancer of exotoxin A expression.", Infect Immun, 61(4), 1180–4.

[48] Gambello M. J., Iglewski B. H., (1991), "Cloning and characterization of the Pseudomonas aeruginosa lasR gene, a transcriptional activator of elastase expression.", J Bacteriol, 173(9), 3000–9.

[49] Pearson J. P., Passador L., Iglewski B. H., Greenberg E. P., (1995), "A second N-acylhomoserine lactone signal produced by Pseudomonas aeruginosa.", Proc Natl Acad Sci U S A, 92(5), 1490–4.

[50] Brint J. M., Ohman D. E., (1995), "Synthesis of multiple exoproducts in Pseudomonas aeruginosa is under the control of RhlR-RhlI, another set of regulators in strain PAO1 with homology to the autoinducer-responsive LuxR-LuxI family.", J Bacteriol, 177(24), 7155–63.

[51] Latifi A., Winson M. K., Foglino M., Bycroft B. W., Stewart G. S., Lazdunski A., Williams P., (1995), "Multiple homologues of LuxR and LuxI control expression of virulence determinants and secondary metabolites through quorum sensing in Pseudomonas aeruginosa PAO1.", Mol Microbiol, 17(2), 333–43.

[52] Ochsner U. A., Koch A. K., Fiechter A., Reiser J., (1994), "Isolation and characterization of a regulatory gene affecting rhamnolipid biosurfactant synthesis in Pseudomonas aeruginosa.", J Bacteriol, 176(7), 2044–54.

[53] Pierson Iii L. S., Pierson E. A., (1996), "Phenazine antibiotic production in Pseudomonas aureofaciens: role in rhizosphere ecology and pathogen

suppression", FEMS Microbiol Lett, 36.

[54] Nasser W., Bouillant M. L., Salmond G., Reverchon S., (1998), "Characterization of the Erwinia chrysanthemi expI-expR locus directing the synthesis of two N-acyl-homoserine lactone signal molecules.", Mol Microbiol, 29(6), 1391–405.

[55] Reverchon S., Bouillant M. L., Salmond G., Nasser W., (1998), "Integration of the quorum-sensing system in the regulatory networks controlling virulence factor synthesis in Erwinia chrysanthemi", Mol Microbiol, 29(6), 1407–1418.

[56] Swift S., Karlyshev A. V, Fish L., Durant E. L., Winson M. K., Chhabra S. R., Williams P., Macintyre S., Stewart G. S., (1997), "Quorum sensing in Aeromonas hydrophila and Aeromonas salmonicida: identification of the LuxRI homologs AhyRI and AsaRI and their cognate N-acylhomoserine lactone signal molecules.", J Bacteriol, 179(17), 5271–81.

[57] Schultz D., Wolynes P. G., Jacob E. Ben, Onuchic J. N., "Deciding fate in adverse times: Sporulation and competence in Bacillus subtilis".

[58] Shanker E., Federle M. J., (2017), "Quorum Sensing Regulation of Competence and Bacteriocins in Streptococcus pneumoniae and mutans.", Genes (Basel), 8(1).

[59] Yarwood J. M., Bartels D. J., Volper E. M., Greenberg E. P., (2004), "Quorum Sensing in Staphylococcus aureus Biofilms", J Bacteriol, 186(6), 1838–1850.

[60] Dunny G. M., (2007), "The peptide pheromone-inducible conjugation system of Enterococcus faecalis plasmid pCF10: cell-cell signalling, gene transfer, complexity and evolution.", Philos Trans R Soc Lond B Biol Sci, 362(1483), 1185–93.

[61] Marques J. C., Lamosa P., Russell C., Ventura R., Maycock C., Semmelhack M. F., Miller S. T., Xavier K. B., (2011), "Processing the interspecies quorum-sensing signal autoinducer-2 (AI-2): characterization of phospho-(S)-4,5-dihydroxy-2,3-pentanedione isomerization by LsrG protein.", J Biol Chem, 286(20), 18331–43.

[62] Xavier K. B., Bassler B. L., (2003), "LuxS quorum sensing: more than just a numbers game", Curr Opin Microbiol, 6(2), 191–197.

[63] Day W. A., Maurelli A. T., Maurelli A. T., (2001), "Shigella flexneri LuxS quorum-sensing system modulates virB expression but is not essential for virulence.", Infect Immun, 69(1), 15–23.

[64] Whitehead N. A., Barnard A. M., Slater H., Simpson N. J., Salmond G. P., (2001), "Quorum-sensing in Gram-negative bacteria.", FEMS Microbiol Rev, 25(4), 365–404.

[65] Blakytny R., Jude E., (2006), "The molecular biology of chronic wounds and

delayed healing in diabetes", Diabet Med, 23(6), 594–608.

[66] Frykberg R. G., Banks J., (2015), "Challenges in the Treatment of Chronic Wounds", Adv Wound Care, 4(9), 560–582.

[67] Zhao G., Usui M. L., Lippman S. I., James G. A., Stewart P. S., Fleckman P., Olerud J. E., (2013), "Biofilms and Inflammation in Chronic Wounds", Adv Wound Care, 2(7), 389–399.

[68] Abraham W.-R., (2006), "Controlling biofilms of gram-positive pathogenic bacteria.", Curr Med Chem, 13(13), 1509–24.

[69] Harrison-Balestra C., Cazzaniga A. L., Davis S. C., Mertz P. M., (2003), "A wound-isolated Pseudomonas aeruginosa grows a biofilm in vitro within 10 hours and is visualized by light microscopy.", Dermatol Surg, 29(6), 631–5.

[70] Williams H. D., Zlosnik J. E. A., Ryall B., (2006), "Oxygen, Cyanide and Energy Generation in the Cystic Fibrosis Pathogen Pseudomonas aeruginosa". In: Advances in microbial physiology. pp 1–71.

[71] Mesaros N., Nordmann P., Plésiat P., Roussel-Delvallez M., Van Eldere J., Glupczynski Y., Van Laethem Y., Jacobs F., Lebecque P., Malfroot A., Tulkens P. M., Van Bambeke F., (2007), "Pseudomonas aeruginosa: Resistance and therapeutic options at the turn of the new millennium", Clin Microbiol Infect, 13(6), 560–578.

[72] Klockgether J., Cramer N., Wiehlmann L., Davenport C. F., Tümmler B., (2011), "Pseudomonas aeruginosa genomic structure and diversity", Front Microbiol, 2(JULY).

[73] Klapper I., Dockery J., "Mathematical Description of Microbial Biofilms *"52(2), 0–0.

[74] Davies D. G., Parsek M. R., Pearson J. P., Iglewski B. H., Costerton J. W., Greenberg E. P., (1998), "The involvement of cell-to-cell signals in the development of a bacterial biofilm.", Science, 280(5361), 295–8.

[75] Schenck L. P., Surette M. G., Bowdish D. M. E., (2016), "Composition and immunological significance of the upper respiratory tract microbiota", FEBS Lett, 590(21), 3705–3720.

[76] Curran J. P., Al-Salihi F. L., (1980), "Neonatal staphylococcal scalded skin syndrome: massive outbreak due to an unusual phage type.", Pediatrics, 66(2), 285–90.

[77] Archer N. K., Mazaitis M. J., William Costerton J., Leid J. G., Powers M. E., Shirtliff M. E., (2011), "Staphylococcus aureus biofilms: Properties, regulation and roles in human disease". Virulence 2:445–459.

[78] Yarwood J. M., Bartels D. J., Volper E. M., Greenberg E. P., (2004), "Quorum

Sensing in Staphylococcus aureus Biofilms", J Bacteriol, 186(6), 1838–1850.

[79] Nguyen A. T., Oglesby-Sherrouse A. G., (2016), "Interactions between Pseudomonas aeruginosa and Staphylococcus aureus during co-cultivations and polymicrobial infections", Appl Microbiol Biotechnol, 100(14), 6141–6148.

[80] Machan Z. A., Taylor G. W., Pitt T. L., Cole P. J., Wilson R., (1992), "2-Heptyl-4-hydroxyquinoline N-oxide, an antistaphylococcal agent produced by Pseudomonas aeruginosa", J Antimicrob Chemother, 30(5), 615–623.

[81] Zhu H., Huang S., Dhar P., (2004), "The next step in systems biology: simulating the temporospatial dynamics of molecular network", BioEssays, 26, 68–72.

[82] Chang D. C., Dokos S., Lovell N. H., (2011), "Temporo-Spatial Model Construction Using the MML and Software Framework", IEEE Trans Biomed Eng, 58(12), 3528–3531.

[83] Macklin P., Edgerton M. E., Thompson A. M., Cristini V., Macklin ", Edgerton P., Thompson M. E., Cristini A., "Patient-calibrated agent-based modelling of ductal carcinoma in situ (DCIS): From microscopic measurements to macroscopic predictions of clinical progression". doi: 10.1016/j.jtbi.2012.02.002".

[84] Chuang H. Y., Hofree M., Ideker T., (2010), "A decade of systems biology - figür". Annu. Rev. Cell Dev. Biol. 26:721–744.

[85] Pavlopoulos G. A., Secrier M., Moschopoulos C. N., Soldatos T. G., Kossida S., Aerts J., Schneider R., Bagos P. G., (2011), "Using graph theory to analyze biological networks.", BioData Min, 4, 10.

[86] Terzer M., Maynard N. D., Covert M. W., Stelling J., (2009), "Genome-scale metabolic networks", Wiley Interdiscip Rev Syst Biol Med, 1(3), 285–297.

[87] Mo M. L., Jamshidi N., Palsson B., (2007), "A genome-scale, constraint-based approach to systems biology of human metabolism", Mol Biosyst, 3(9), 598–603.

[88] Chaouiya C., Bérenguier D., Keating S. M., Naldi A., van Iersel M. P., Rodriguez N., Dräger A., Büchel F., Cokelaer T., Kowal B., Wicks B., Gonçalves E., Dorier J., Page M., Monteiro P. T., von Kamp A., Xenarios I., de Jong H., Hucka M., Klamt S., Thieffry D., Le Novère N., Saez-Rodriguez J., Helikar T., (2013), "SBML qualitative models: a model representation format and infrastructure to foster interactions between qualitative modelling formalisms and tools", BMC Syst Biol, 7(1), 135.

[89] Li C., Donizelli M., Rodriguez N., Dharuri H., Endler L., Chelliah V., Li L., He E., Henry A., Stefan M. I., Snoep J. L., Hucka M., Le Novère N., Laibe C., (2010), "BioModels Database: An enhanced, curated and annotated resource for published quantitative kinetic models", BMC Syst Biol, 4(1), 92.

[90] Noronha A., Modamio J., Jarosz Y., Sompairac N., Gonzalez G. P., Danielsdottir A. D., Krecke M., Merten D., Haraldsdottir H. S., Heinken A., Heirendt L., Magnusdottir S., Ravcheev D. A., Sahoo S., Gawron P., Guerard E., Fiscioni L., Garcia B., Prendergast M., Puente A., Rodrigues M., Roy A., Rouquaya M., Wiltgen L., Zagare A., John E., Krueger M., Kuperstein I., Zinovyev A., Schneider R., Fleming R. M. T., Thiele I., (2018), "The Virtual Metabolic Human database: integrating human and gut microbiome metabolism with nutrition and disease", bioRxiv, 321331.

[91] Becker S. A., Palsson B. O., (2008), "Context-specific metabolic networks are consistent with experiments.", PLoS Comput Biol, 4(5), e1000082.

[92] Agren R., Bordel S., Mardinoglu A., Pornputtapong N., Nookaew I., Nielsen J., (2012), "Reconstruction of Genome-Scale Active Metabolic Networks for 69 Human Cell Types and 16 Cancer Types Using INIT", PLoS Comput Biol, 8(5), e1002518.

[93] Colijn C., Brandes A., Zucker J., Lun D. S., Weiner B., Farhat M. R., Cheng T.-Y., Moody D. B., Murray M., Galagan J. E., (2009), "Interpreting Expression Data with Metabolic Flux Models: Predicting Mycobacterium tuberculosis Mycolic Acid Production", PLoS Comput Biol, 5(8), e1000489.

[94] Zur H., Ruppin E., Shlomi T., (2010), "iMAT: an integrative metabolic analysis tool", Bioinformatics, 26(24), 3140–3142.

[95] Wang Y., Eddy J. A., Price N. D., (2012), "Reconstruction of genome-scale metabolic models for 126 human tissues using mCADRE", BMC Syst Biol, 6(1), 153.

[96] Phalak P., Chen J., Carlson R. P., Henson M. A., (2016), "Metabolic modeling of a chronic wound biofilm consortium predicts spatial partitioning of bacterial species", BMC Syst Biol, 10(1), 1–20.

[97] Qu Z., Garfinkel A., Weiss J. N., Nivala M., (2011), "Multi-scale modeling in biology: how to bridge the gaps between scales?", Prog Biophys Mol Biol, 107(1), 21–31.

[98] Khan F. M., Marquardt S., Gupta S. K., Knoll S., Schmitz U., Spitschak A., Engelmann D., Vera J., Wolkenhauer O., Pützer B. M., (2017), "Unraveling a tumor type-specific regulatory core underlying E2F1-mediated epithelial-mesenchymal transition to predict receptor protein signatures", Nat Commun, 8(1), 198.

[99] Hoops S., Sahle S., Gauges R., Lee C., Pahle J., Simus N., Singhal M., Xu L., Mendes P., Kummer U., (2006), "COPASI--a COmplex PAthway SImulator", Bioinformatics, 22(24), 3067–3074.

[100] Hoekstra A. G., Falcone J.-L., Caiazzo A., Chopard B., (2008), "Multi-scale Modeling with Cellular Automata: The Complex Automata Approach". In: Cellular Automata. Springer Berlin Heidelberg, Berlin, Heidelberg, pp 192–

199.

[101] Ghaemi M., Shahrokhi A., "Combination of The Cellular Potts Model and Lattice Gas Cellular Automata For Simulating The Avascular Cancer Growth".

[102] Graner F., Glazier J. A., (1992), "Simulation of biological cell sorting using a two-dimensional extended Potts model", Phys Rev Lett, 69(13), 2013–2016.

[103] Mirams G. R., Arthurs C. J., Bernabeu M. O., Bordas R., Cooper J., Corrias A., Davit Y., Dunn S.-J., Fletcher A. G., Harvey D. G., Marsh M. E., Osborne J. M., Pathmanathan P., Pitt-Francis J., Southern J., Zemzemi N., Gavaghan D. J., (2013), "Chaste: An Open Source C++ Library for Computational Physiology and Biology", PLoS Comput Biol, 9(3), e1002970.

[104] Starruß J., de Back W., Brusch L., Deutsch A., (2014), "Morpheus: a user-friendly modeling environment for multiscale and multicellular systems biology.", Bioinformatics, 30(9), 1331–2.

[105] Swat M. H., Thomas G. L., Belmonte J. M., Shirinifard A., Hmeljak D., Glazier J. A., (2012), "Multi-Scale Modeling of Tissues Using CompuCell3D", Methods Cell Biol, 110, 325–366.

[106] Bauer E., Zimmermann J., Baldini F., Thiele I., Kaleta C., (2017), "BacArena: Individual-based metabolic modeling of heterogeneous microbes in complex communities", PLOS Comput Biol, 13(5), e1005544.

[107] Ghaffarizadeh A., Friedman S. H., Macklin P., (2016), "BioFVM: an efficient, parallelized diffusive transport solver for 3-D biological simulations", Bioinformatics, 32(8), 1256–1258.

[108] Ghaffarizadeh A., Friedman S. H., Mumenthaler S. M., Macklin P., (2016), "PhysiCell: an Open Source Physics-Based Cell Simulator for 3-D Multicellular Systems". doi: 10.1101/088773.

[109] Stewart P. S., (2003), "Diffusion in biofilms.", J Bacteriol, 185(5), 1485–91.

[110] Groenendaal W., Schmidt K. A., Von Basum G., Van Riel N. A. W., Hilbers P. A. J., (2008), "Modeling glucose and water dynamics in human skin", Diabetes Technol Ther, 10(4), 283–293.

[111] Oberhardt M. A., Puchałka J., Fryer K. E., Martins dos Santos V. A. P., Papin J. A., (2008), "Genome-scale metabolic network analysis of the opportunistic pathogen Pseudomonas aeruginosa PAO1.", J Bacteriol, 190(8), 2790–803.

[112] M H., A K., R R., S P., (2005), "In silico genome-scale reconstruction and validation of the Staphylococcus aureus metabolic network", Biotechnol Bioeng, 92(7), 850–864.

[113] Ebrahim A., Lerman J. A., Palsson B. O., Hyduke D. R., (2013), "COBRApy: COnstraints-Based Reconstruction and Analysis for Python".

[114] Orth J. D., Thiele I., Palsson B. Ø., (2010), "What is flux balance analysis?", Nat Biotechnol, 28(3), 245–8.

[115] Wishart D. S., Tzur D., Knox C., Eisner R., Guo A. C., Young N., Cheng D., Jewell K., Arndt D., Sawhney S., Fung C., Nikolai L., Lewis M., Coutouly M. A., Forsythe I., Tang P., Shrivastava S., Jeroncic K., Stothard P., Amegbey G., Block D., Hau D. D., Wagner J., Miniaci J., Clements M., Gebremedhin M., Guo N., Zhang Y., Duggan G. E., MacInnis G. D., Weljie A. M., Dowlatabadi R., Bamforth F., Clive D., Greiner R., Li L., Marrie T., Sykes B. D., Vogel H. J., Querengesser L., (2007), "HMDB: The human metabolome database", Nucleic Acids Res, 35(SUPPL. 1).

[116] Lin L., Bhawana R., Xue Y., Duan Q., Jiang R., Chen H., Chen X., Sun B., Lin H., (2018), "Comparative analysis of diffusional kurtosis imaging, diffusion tensor imaging, and diffusion-weighted imaging in grading and assessing cellular proliferation of meningiomas", Am J Neuroradiol, 39(6), 1032–1038.

[117] Skindersoe M. E., Alhede M., Phipps R., Yang L., Jensen P. O., Rasmussen T. B., Bjarnsholt T., Tolker-Nielsen T., Høiby N., Givskov M., (2008), "Effects of Antibiotics on Quorum Sensing in Pseudomonas aeruginosa", Antimicrob Agents Chemother, 52(10), 3648.

[118] Wagner V. E., Bushnell D., Passador L., Brooks A. I., Iglewski B. H., (2003), "Microarray Analysis of Pseudomonas aeruginosa Quorum-Sensing Regulons: Effects of Growth Phase and Environment", J Bacteriol, 185(7), 2080.

[119] Consortium G. O., (2004), "The Gene Ontology (GO) database and informatics resource", Nucleic Acids Res, 32(suppl_1), D258–D261.

[120] Mi H., Muruganujan A., Casagrande J. T., Thomas P. D., (2013), "Large-scale gene function analysis with the PANTHER classification system", Nat Protoc 2013 88, 8(8), 1551–1566.

[121] Goo E., An J. H., Kang Y., Hwang I., (2015), "Control of bacterial metabolism by quorum sensing". Trends Microbiol. 23:567–576.

[122] Stewart P. S., (2003), "Diffusion in biofilms". J. Bacteriol. 185:1485–1491.

[123] Angeles Bonafonte M., Solano C., Alvarez M., Montuenga L., Garc D., Gamazo aY C., "The relationship between glycogen synthesis, biofilm formation and virulence in Salmonella enteritidis".

[124] Yang L., Haagensen J. A. J., Jelsbak L., Johansen H. K., Sternberg C., Høiby N., Molin S., (2008), "In situ growth rates and biofilm development of Pseudomonas aeruginosa populations in chronic lung infections", J Bacteriol, 190(8), 2767–2776.

[125] White B. M., (2016), "Understanding the physiology of Pseudomonas aeruginosa biofilms in an in vitro chronic wound model" , Master's Thesis, Montana State University.

[126] Ramos I., Dietrich L. E. P., Price-Whelan A., Newman D. K., (2010), "Phenazines affect biofilm formation by Pseudomonas aeruginosa in similar ways at various scales", Res Microbiol, 161(3), 187–191.

[127] Felig P., Wahren J., Sherwin R., Palaiologos G., (1977), "Amino Acid and Protein Metabolism in Diabetes Mellitus", Arch Intern Med, 137(4), 507–513.

[128] Serra R., Grande R., Butrico L., Rossi A., Settimio U. F., Caroleo B., Amato B., Gallelli L., De Franciscis S., (2015), "Chronic wound infections: The role of Pseudomonas aeruginosa and Staphylococcus aureus". Expert Rev. Anti. Infect. Ther. 13:605–613.

[129] Jeannotte R., (2014), "METABOLIC PATHWAYS | Nitrogen Metabolism", Encycl Food Microbiol Second Ed, 544–560.

[130] Schmid N., Pessi G., Deng Y., Aguilar C., Carlier A. L., Grunau A., Omasits U., Zhang L. H., Ahrens C. H., Eberl L., (2012), "The AHL- and BDSF-Dependent Quorum Sensing Systems Control Specific and Overlapping Sets of Genes in Burkholderia cenocepacia H111", PLoS One, 7(11), 49966.

[131] Chen B., Wen J., Zhao X., Ding J., Qi G., (2020), "Surfactin: A Quorum-Sensing Signal Molecule to Relieve CCR in Bacillus amyloliquefaciens", Front Microbiol, 11, 631.

BIOGRAPHY

Tuğberk Talak completed his undergraduate studies in Mathematics at Gebze Technical University. In 2018, he started to study for his master's degree in Bioinformatics and Systems Biology Programme in the same university. He participated in 116S388 research project funded by TUBITAK and TÜSEB-2019-TA-01 research project funded by TÜSEB during his master's education.